NEW METHOD FOR TESTING THE DYNAMIC CUTTING FORCE COEFFICIENTS

NEW METHOD FOR TESTING THE DYNAMIC CUTTING FORCE COEFFICIENTS

By

O. HECZKO, Dipl. Ing.

A Thesis

Submitted to the School of Graduate Studies

in Partial Fulfilment of the Requirement

for the Degree

Master of Engineering

McMaster University

July 1980

MASTER OF ENGINEERING (1980) McMASTER UNIVERSITY
Hamilton, Ontario

TITLE: New Method for Testing the Dynamic Cutting Force Coefficients

AUTHOR: Oskar Heczko, Dipl. Ing.
(Technical University of Ostrava, Czechoslovakia, 1965)

SUPERVISOR: Professor Dr. J. Tlusty

NUMBER OF PAGES: xii , 101

ABSTRACT

The dynamic behaviour of metal cutting process is investigated by measuring the Dynamic Cutting Force Coefficients. Measurements of eight components of the DCFC's are needed to describe completely the dynamics of metal cutting. This requires complex test apparatus and procedures, yet the experimental results are not very convincing.

Investigations of the DCFC's for the inner modulation only, as recommended by Tlusty on CIRP in 1978, simplified the problem.

A new method has been developed for measuring the inner DCFC's. The new method is based on Kal's idea who compared transient vibrations of a test rig in the cut with that outside the cut, which provides a direct assessment of the damping in the cutting process. New arrangements of the test and especially, the controlability of the damping of the rig itself leads to a qualitatively new situation permitting a high level of sensitivity and distinction of slight variations in the damping of the cutting process.

The experimental results obtained by the new method are very convincing and are in a very good agreement with the general practical observations.

ACKNOWLEDGEMENTS

The author wishes to acknowledge with deep gratitude the assistance of those who contributed to the completion of this work. He is particularly grateful to his supervisor, Dr. J. Tlusty, Professor of Mechanical Engineering, for his guidance and advice throughout the course of the work.

Appreciation is extended to the National Research Council of Canada and to the Department of Mechanical Engineering at McMaster University for their financial assistance.

Finally, the author would like to thank Mrs. Gillian Wood for typing the manuscript.

TABLE OF CONTENTS

TABLE OF CONTENTS
(cont'd)

LIST OF ILLUSTRATIONS

LIST OF ILLUSTRATIONS
(cont'd)

NOMENCLATURE

$A_{(o,n)}$	Amplitude of vibration
$A_{(n,t)}$	Complex cutting force coefficient of inner modulation for normal resp. tangential force
$B_{(n,t)}$	Complex cutting force coefficient of outer modulation for normal respective tangential force
b	Width of cut
b_{lim}	Limit width of cut
$C_{(1,2)}$	Capacitance.
c	Damping coefficient of the system
c_c	Damping coefficient of total machining system
c_{cr}	Critical damping
c_i	Specific process damping
c_p	Damping coefficient of cutting process
D	Universal machinability index
$F_{(n,t)}$	Dynamic component of normal cutting force respective tangential cutting force
$F_{v(i,o)}$	Dynamic component of main cutting force for inner respective outer modulation
$F_{p(i,o)}$	Dynamic component of thrust cutting force for inner respective outer modulation
F_o	Dynamic component of cutting force
$\Delta F_{\mathcal{L}}$	Dynamic component projection of resultant cutting force
f	Frequency
$G(\omega)$	Real part of transferfunction of machine tool structure

G_{min}	Minimum value of $G(\omega)$
$G_{(d,c)}$	Transferfunction of machine tool structure - direct respective cross
$H_{(w)}$	Imaginary part of transferfunction of machine tool structure
Δh	Increment of chip thickness
j	$\sqrt{-1}$
$K_{c(1,o)}$	Complex cross dynamic cutting force coefficient for inner respective outer modulation
$K_{d(i,o)}$	Complex direct dynamic cutting force coefficient for inner respective outer modulation
$K_{(t,r)}$	Total stiffness respective stiffness of rig
$K_{\alpha\alpha}$	Direct stiffness
$K_{\alpha\beta}$	Cross stiffness
k	Stiffness of system
k_c	Stiffness of total machining system
k_i	Incremental stiffness, specific process stiffness
k_p	Stiffness of cutting process
ℓ	Shear plane length
ℓ_s	Instantaneous shear plane length
m	Mass, mass of test rig
N	Integer, rotational speed
n	Integer
R	Coefficient of coupling intensity
$R_{(1,2)}$	Resistance
r	Coefficient, stiffness
s	$j\omega$, feed rate
$u_{(c,d)}$	Directional factor - cross respective direct

v	Cutting speed, voltage
$v_{(i,o)}$	Input voltage respective output voltage
W	Wavelength
X	Amplitude of displacement
$Y_{(o)}$	Chip thickness modulation - inner respective outer
Y	Direct chip thickness modulation
α	Angle between principal direction of motion and direction of chip thickness modulation, rake angle
β	Angle between k_i and direction perpendicular to cut surface, angle between principal direction of motion and direction of chip thickness modulation
γ	Angle between c_i and direction perpendicular to cut surface, clearance angle
δ	Phase angle between shear plane length variation and uncut chip thickness variation, phase shift between force vector and modulation
ϵ	Phase angle between inner and outer modulations
ϕ	Phase angle
λ	Logarithmic decrement
ξ	Damping ratio of system
ξ_c	Damping ratio of system when cutting
ω	Angular frequency, natural frequency of test rig
ω_c	Angular frequency of test rig when cutting
ω_n	Angular natural frequency

CHAPTER I

INTRODUCTION

Different kinds of vibrations often occur during machining of metals. These vibrations tend to produce more or less periodical deviations in the modulations of the machined surface to a certain extent. Noise, increasing of tool wear, bad surface quality and even unstable cutting process can be the result of these vibrations. From their nature it is possible to distinguish two major kinds of vibrations:

- forced vibrations and
- vibrations generated by the cutting process itself.

Forced vibrations are usually caused by any unbalance in the gears, irregularities in driving elements, guide ways, hydraulic devices, or by an electrical unbalance. They can be transmitted from other sources through the foundations too.

Vibrations generated by the cutting process itself can be divided into two classes:

- free vibrations and

- self-excited vibrations

Free vibrations are of transient nature and are damped usually in a very short period of time depending on the damping available in the machining system. They can be caused by any interruption in the cutting process, such as a slot in the workpiece, hard particles in the workpiece material or instability of the built-up edge. However, they are of minor importance.

Self-excited vibrations are referred to as "chatter" in metal cutting and as mentioned above they belong to the class of vibrations induced by the cutting process alone. The energy generated in the cutting process excites the machine structure to undergo vibrating motion; the motion itself leads to further vibratory energy being generated in the cutting process. Once chatter starts the amplitude of vibration usually increases to an extremely violent level. The frequencies for this type of vibration are approximately equal to the natural frequencies of the machine tool structure. Detail consideration is provided in Chapter 3.

The changes in the cutting conditions, reducing of cutting speed or width of cut or even stopping of machining, are the only ways to overcome chattering and to

install stable machining.

With the advent of numerically controlled machine tools the problem of chatter has become even more complicated. The changes in the cutting conditions as mentioned above cannot be applied for overcoming chatter, should it start during machining. Moreover, with the necessity of machines having to operate at the optimum conditions, the problem of chatter has attained great significance. There is a need to develop the ability to predict the cutting conditions under which chatter cannot occur and which could lead to stable machining.

There are two ways to tackle the problem of stable machining. Firstly, studying the cutting conditions of chatter. Secondly, defining rules for the design of machine tools with higher stability. Or, in other words, studying transferfunctions of the cutting process and of the machine tool system.

In the past, successful techniques (1, 2) have been developed for measuring the transferfunction of the machine tool system. However, they are not the subject of study of this work.

Although considerable research effort has been

devoted to the investigation of the transferfunction of the cutting process which is actually represented by the Dynamic Cutting Force Coefficients, no firm result has yet been satisfactorily established. The complex test apparatus and procedures were one of reasons for this lack of success.

The data generated in the cooperative CIRP project by laboratories in Aachen, Leuven, Prague and McMaster (3, 4) were assembled in (7). They represent practically the first data obtained under real cutting conditions. However, they represent data for one steel CK45N (equivalent to 1045 normalized) only. Big discrepancies have been experienced especially in the imaginary direct inner coefficient Im (K_{di}), which is the most important parameter.

There was a general feeling that one way to success would be in the simplification of the problem. Tlusty (7) presented in the discussion on the CIRP in 1978 an analysis showing that one of the eight components of the DCFCs is most significant and some of them have no practical value. The theoretical part regarding the stability is outlined in Chapter 3.

The work presented here is an attempt of reviving and modifying one of the simplest and most straightforward

methods. It was suggested and investigated in 1971 by Kals (5, 6). A new approach is based on the measurement of the damping due to the inner modulation only and using a set-up which excludes regeneration of surface waviness. The main advantage of this method is seen in the directly interpretable measurements. Damping in the cutting process is related to changes in the rate of decay of transient vibrations of a cutting tool attached to the test rig.

Correspondingly, the objectives of this work can be defined as follows:

1. To develop a simple method of measurement of the inner modulation DCFCs which would supply values for the damping in the cutting process with an improved repeatability and with a reliable conformity with stability of cutting observed in practical operations. As a target repeatability of ∓ 20% is set.

   The method should be based on the original method of Kals. However, changes are necessary so as to improve its repeatability.

2. To use the new method and obtain values of the inner modulation DCFCs for two different steels and for one aluminium alloy.

CHAPTER II

LITERATURE SURVEY

The experimental methods used to obtain the transfer function of the cutting process can be subdivided into two main groups:

- the static methods
- the dynamic methods

The static methods are based on measurements of static force components. They are easy to perform but they give only indirect and incomplete answers to the dynamic problem, because of assuming a certain model.

The dynamic methods use a vibratory tool excited either by a pulse (impact) or with sinusoidal signal. They allow for direct observation of the dynamic components. The problem is that they require an elaborate instrumentation.

Considering the complexity of the problem, the orthogonal cutting is usually applied to reduce the geometric problem to a plain one. In all cases a lathe was used for conducting the experiment.

2.1 Static-methods

Tobias and Fischwick (13) tried in a more complicated way to express the incremental force.

In the low range of cutting speed the stability is higher compared with middle and high ranges of cutting speed. The increased stability was explained by postulating that cutting process damps the motion between the tool and the workpiece. They called it "the penetration effect". Finally, they proposed the cutting force equation in which influence of chip thickness, rate of penetration and cutting speed are incorporated

$$F = b\ (k_1 ds + k_2 dr + k_3 d\Omega) \qquad 2.1$$

where ds, dr and $d\Omega$ are variations in the chip thickness, rate of penetration and cutting speed. The dynamic coefficients were related to steady state cutting coefficents k_s and k_Ω

$$k_2 = \frac{2\pi(k_s - k_1)}{\Omega} \qquad 2.2$$

$$k_3 = k_\Omega - \frac{k_s - k_1}{\Omega} \qquad 2.3$$

where k_s was determined from the slope of the force-feed relationship, k_Ω determined from the slope of the force-speed relationship and k_1 being determined from dynamic cutting experiments.

About the mean cutting conditions k_s and k_Ω were taken as constants. The dependency of cutting form on cutting speed was neglected and equation (2.1) was written as:

$$F = b\ (k_1 ds + k_2 dr) \qquad 2.4$$

Comparing (2.4) and (3.3) it can be seen that k_1 and r are initially the same, equation (2.4) is probably more exact because of the attempt to express the damping.

Steady state was the basis at which dynamic coefficients were obtained. Such a concept cannot fully describe the cutting process. This was a first try to express damping. Since then researchers began to investigate the process under chatter conditions.

Das and Tobias (14) developed a mathematical model of regenerative cutting process in which shear plane theory combined with inner and outer modulations were applied. The effect of both modulations was studied independently. They approached the problem from the point of the geometry of cutting process, the expression for steady state cutting forces were modified to incorporate the cyclic variations of different cutting parameters. The arguments leading to the expressions for various components of the

dynamic cutting force are as follows.

The steady state cutting force:

$$f_v = k_c b \ell \qquad 2.5$$

$$f_p = k_c b \ell \left(\frac{D \cos\phi - 1}{D \sin\phi}\right) \qquad 2.6$$

where b = chip width

k_c = the slope of f_v and shear plane area

ϕ = shear plane angle

ℓ = length of shear plane

D = Universal Machinability Index

For the wave cutting (inner modulation), the shear plane length undergoes cyclic variation because of tool vibration, the instantaneous shear plane length is given by the equation:

$$p_s = \frac{s + ds \sin \omega t}{\sin\phi} \qquad 2.7$$

And for wave removing (outer modulation) the instantaneous shear plane length is given by the equation:

$$\ell s = \frac{ds (\sin \omega t + \delta_o)}{\sin\phi} \qquad 2.8$$

Where s is the nominal depth on the feed rate, ds is the variation in depth of cut due to tool vibration and δ is the phase angle between the shear plane length variation and uncut chip thickness.

A direct substitution of equations (2.7, 2.8) into equations (2.5,2.6) gives the total static and dynamic parts of cutting force components along and perpendicular to the instantaneous direction of cutting for inner and outer modulation.

Only the dynamic force components are considered and are as follows:

$$F_{vi} = dF_{co} \sin(\omega t + \delta vi) \qquad 2.9$$

$$F_{pi} = dF_{to} \sin(\omega t + \delta pi) \qquad 2.10$$

$$Fvo = k_{ic}\, ds\, (\sin \omega t + \delta o) \qquad 2.11$$

$$Fpo = k_{it}\, ds\, (\sin \omega t + \delta o) \qquad 2.12$$

where dF_{co} dF_{to}, S, k_{ic}, k_{it} are functions of D, ϕ, V, S and k_c.

The concept of this work was again based on the steady state conception. Using such a concept has been proved to be doubtful, because it unables to express the damping generated by the cutting process.

The most important point of this work is the concept of independent behaviour of inner and outer modulation.

Peters and Vanhereck's (15) work was based on the

assumption of using the incremental cutting stiffness k_i for the already mentioned r value. Thus, they calculated the critical width of cut by using the equation (3.9) proposed by Tlusty (8).

$$b_{lim} = \frac{1}{2\ k_i(-Re(G_{min}))} \qquad 2.13$$

The values of k_i were obtained by static cutting tests. The static stiffness was determined from the ratio of incremental cutting force ΔF to the increment in the chip thickness Δh for main and thrust cutting forces, Fig. 8.1. The incremental cutting stiffness was defined as:

$$k_i = k_{st} \cos \beta \qquad 2.14$$

$$k_{st} = \frac{\Delta F}{\Delta h} \qquad 2.15$$

where β represented the angle between the vector ΔF and the direction of motion of the tool.

Various cutting conditions (cutting speed, feed rate) were used to obtain the values of k_i. And finally b_{lim} was calculated for a single degree of freedom structure which G_{min} was exactly defined. The calculated b_{lim} values and the experimentally obtained b_{lim} values for the given rig were compared and a fairly good resemblance was found.

However, similar experiments carried out at

Eindhoven (5), using the same rig, showed larger discrepencies.

As was mentioned to the first method, the technique used by Peters and Vanhereck was inadequate for studying of cutting process.

2.2 Dynamic methods

The dynamic methods can be subdivided into two groups:

- the dynamometer methods
- the stiffness methods

3.2.1 Dynamometer methods

Polacek (10) devised an experimental technique for measuring the forces for outer and inner modulation. This is a simulating conditions under regenerative chatter. The tool is mounted on a dynamometer. The rig (set up) vibrates by means of an exciter. Firstly the dynamometer had to be compensated on the dynamic response. Secondly it had to be kept track of outer modulation, which was done by driving the spindle with a synchronous motor and storing the outer modulation on a magnetic disc.

The instantaneous chip thickness was obtained from the difference between the current displacement of the tool

and tool displacement at exactly one revolution earlier. The frequency can be written as:

$$f = (k + \frac{\varepsilon}{2\pi}) \frac{N}{60} \qquad 2.16$$

where N - rotational speed

ε - the phase between inner and outer modulation

k - an integer

The dynamic force components F_f and F_v were measured in the normal (feed) and tangential (cutting speed) directions respectively. Taking e.g. F_f, (Fig. 8.2), it is possible to draw it in the complex plane. When the experiment is repeated for different ε values, the vector describes a circle around a center S which is fixed and located somewhere in the complex plane. Consequently it is possible to decompose F_t in two components: One of those F_{fi} steadily oriented toward S, the other one F_{fo} rotating around S, synchronously but not in phase with outer modulation h_o. Each can be decomposed in an inphase and a quadrature component with respect to their chip thickness modulation. They are Re (F_{fi}), Im (F_{fi}), Re (F_{fo}), Im (F_{fo}). The same procedure is done with tangential fore F_v.

Opitz and Werntze (9) developed an experimental technique to measure the DCFC's by taking the signals of

cutting force and tool displacement using a two component cutting force dynamometer and capacitive probe respectively and recording them in a process control computer. The rig was of one degree of freedom.

The signals were processed digitally to obtain dynamic coefficients, chip thickness variation, phase shift between force components and chip thickness and phase shift between inner and outer modulations. DCFC's were given as a ratio of cutting force component to the chip thickness variation together with the phase shift between these quantities. The set-up did not allow any control over the phase shift 'ε' between inner and outer modulation. The phase shift was measured by comparing signals of tool displacement at the current revolution of the workpiece and the previous revolution. The coordination of the two signals was done by using a shift encoder mounted at the end of the lathe spindle to control the digitization process for each revolution. They reported that no significant changes in the phase shift were found for the period in which the signals were taken.

Various cutting conditions and the effect of the phase shift 'ε' between inner and outer modulation were investigated. It was found that the main cutting force led,

slightly, the chip thickness variation and was constant over the whole range of 'ε' while considerable change was observed in the phase shift of the thrust cutting force. A significant variation of DCFC's was observed as the cutting speed was varied. The variations in feed rate or excitation frequency showed no significant influence on DCFC's.

Goel and Tlusty (12, 16) developed the double modulation method which overcomes drawbacks encountered in the previous methods. The regenerative cutting process was analysed on the assumption of independency of the inner and outer modulations. The experiment was executed with a rig of a single degree of freedom on which a two component cutting force dynamometer was mounted (orthogonal cutting process). The dynamometer measured the cutting force components in the normal and tangential directions using piezoelectric force transducers. The tool displacement was measured with a capacitance probe. The force and displacements signals were fed into the Hewlett-Packard Fourier Analyser System.

The cutting tool was continuously excited by an electro-hydraulic exciter. The frequency of excitation was linked to the rotational speed of the workpiece to

control and maintain the phase shift 'ε' between the inner and outer modulations by using a digitizer at the end of the lathe spindle. A synchronous motor was used for driving the spindle.

In view of the independency of the inner and outer modulations, cutting force components could be assigned to both modulations, a detailed model of cutting process was formulated, Fig. 8.3b and since all quantities were varying harmonically with a frequency ω, they could be represented by vectors, see Fig. 8.3a presented for the normal force only. Further the forces F_{ni} and F_{no} were related to their modulations X_i and X_o by coefficients, DCFC's A_n and B_n respectively for a unit width of cut b.

$$F_{ni}e^{j(\omega t + \varsigma_{ni})} = A_n\ b\ X_i e^{j\omega t} \qquad 2.17$$

$$F_{no}e^{j(\omega t + \varsigma_{no})} = B_n\ b\ X_o e^{j\omega t} \qquad 2.18$$

where ς_i, is the phase shift between the force vector and the modulation, the total force is the vectorial difference of F_{ni} and F_{no}

$$F_n e^{j(\omega t + \theta_n)} = b\ (A_n\ x_i e^{j\omega t} - B_n X_o e^{j(\omega t - \varepsilon)}) \qquad 2.19$$

where ε is the phase shift between two modulations and θ_n represents the phase shift of F_n to X_i.

Quantities F_n, X_i and X_o of equation (2.19) are then transformed into vectors represented by complex numbers. The transformed equation (2.19) reduces to a simple algebraic equation:

$$S(F_n) = b\ (A_n S(X_i) - B_n S(X_o) \qquad 2.20$$

where S represents the Fourier transformation of quantities in parenthesis.

For evaluating DCFC A_n and B_n, two equations of the form of equations (2.20) are needed. These can be obtained for different values of the phase shift given ε_1 and ε_2 and giving equations (2.21) and (2.22)

$$S(F_{n1}) = b\ (A_n S(X_{i1}) - B_n S(X_{o1})) \qquad 2.21$$

$$S(F_{n2}) = b\ (A_n S(X_{i2}) - B_n S(X_{o2})) \qquad 2.22$$

Using a simultaneous solution of the above equations gives:

$$A_n = \frac{S(F_{n1}).S(X_{o2}) - S(F_{n2}).S(X_{o1})}{S(X_{i1}).S(X_{o2}) - S(X_{o1}).S(X_{i2})}\ \frac{1}{b} \qquad 2.23$$

$$B_n = \frac{S(F_{n1}).S(X_{i2}) - S(F_{n2}).S(X_{i1})}{S(X_{i1}).S(X_{o2}) - S(X_{o1}).S(X_{i2})}\ \frac{1}{b} \qquad 2.24$$

Coefficients A_n and B_n in general are complex numbers since all the quantities in the R.H.S. of equations (2.23) and (2.24) are complex numbers. A_n and B_n are therefore represented by real and imaginary parts with respect to X_i and X_o as:

$$Re(A_n),\ Im(A_n),\ Re(B_n),\ Im(B_n)$$

Similarly DCFC's for tangential force are obtained with respect to X_i and X_o:

$Re(A_t)$, $Im(A_t)$, $Re(B_t)$, $Im(B_t)$

The same method was used by B.S. Rao (17). He modified the experimental rig used by Goel. Goel's rig could be used for cutting in the longitudinal feed direction only and therefore the tedious manufacture of thin tubes was required. The modification consisted in rebuilding the rig to use in the cross feed direction.

The DCFC's obtained with the new rig were very similar to results obtained by Goel. There were investigations made in the effect of clearance and interferance on cutting forces as well.

Goel and Tlusty's double modulation method overcame drawbacks which were encountered in all other methods. The conducted experiments produced data of the DCFC's for three materials.

2.2.2 Stiffness methods

Peters, Vanhereck, vanBrussel (11) used for their method the CIRP test rig. The rig stiffness is in parallel with cutting process stiffness which is done in virtue of the rig design. This feature allows to get the process

stiffness K_c as a vectorial subtraction. For this purpose the measurement of the total stiffness K_t (test rig and cutting process) during cutting is made whilst the dynamic stiffness of the rig K_r is known from a preliminary measurement. Both direct stiffnesses have to be measured in the model direction of the rig. The method is not valid with cross stiffness. The stiffness is:

$$K_{\alpha\beta} = \frac{F_\alpha}{X_\beta} \qquad 2.25$$

where α, β are angles of directions, F is force and X is a displacement. The direct stiffness $K_{\alpha\alpha}$ is when $\alpha = \beta$, if $\alpha \neq \beta$ the stiffness is called the cross stiffness $K_{\alpha\beta}$. The process stiffness is:

$$K_{c\alpha\alpha} = K_{t\alpha\alpha} - K_{r\alpha\alpha} = \frac{F_{t\alpha}}{X_{t\alpha}} = \frac{F_{r\alpha}}{X_{r\alpha}} \qquad 2.26$$

Stiffness is not a space oriented vector but a complex quantity with a real and an imaginary component, see Fig. 8.4.

The method is based on the assumption that inner and outer modulation are independent. The inner and outer modulation are linked as follows: the harmonic exciter frequency and phase are derived from a disc with holes which is fixed at the end of the lathe spindle. The signal is taken by a photoelectric cell and processed electronically

into a sinusoidal signal of chosen frequency a phase shift $\varepsilon(0 = \varepsilon = 360)$. The direct stiffness $K_{\alpha\alpha}$ for two different ε $(\pi, 2\pi)$ is calculated. A second set of similar measurements has to be done with another rig with model direction β, it gives the direct stiffness $K_{\beta\beta}$ for the same ε values. Every time the in phase and quadrature components are yielded. Further, the stiffness of the rig is subtracted vectorially from the total stiffness. From this eight values are given:

$$R_e(K_{\alpha\alpha\pi}) \quad I_m(K_{\alpha\alpha\pi}) \quad R_e(K_{\alpha\alpha 2\pi}) \quad I_m(K_{\alpha\alpha 2\pi})$$

$$R_e(K_{\beta\beta\pi}) \quad I_m(K_{\beta\beta\pi}) \quad R_e(K_{\beta\beta 2\pi}) \quad I_m(K_{\beta\beta 2\pi})$$

Determination of the phase components of the direct cutting stiffness in a model direction due to the inner and outer modulation are computed vectorially as:

$$R_e(K_{\alpha\alpha})_i = \frac{R_e(K_{\alpha\alpha\pi}) + R_e(K_{\alpha\alpha 2\pi})}{2} \qquad 2.27$$

$$R_e(K_{\alpha\alpha})_o = \frac{R_e(K_{\alpha\alpha\pi}) - R_e(K_{\alpha\alpha 2\pi})}{2} \qquad 2.28$$

$$I_m(K_{\alpha\alpha})_i = \frac{I_m(K_{\alpha\alpha\pi}) + I_m(K_{\alpha\alpha 2\pi})}{2} \qquad 2.29$$

$$I_m(K_{\alpha\alpha})_o = \frac{I_m(K_{\alpha\alpha\pi}) - I_m(K_{\alpha\alpha 2\pi})}{2} \qquad 2.30$$

for the $\alpha\alpha$ direction, the same procedure is applied for the $\beta\beta$ direction.

From the measured direct stiffness components of $K_{\alpha\alpha}$ a $K_{\beta\beta}$ they deducted the corresponding cross stiffness and direct stiffness for the feed direction f and the cutting speed direction v. The experiments on tube cutting showed that only the motion in the feed direction had an influence on the dynamic cutting force. So K_{fv} and K_{vv} were neglected and only K_{ff} and K_{vf} had to be determined.

$$K_{ff} = \frac{1}{2} \frac{K_{\alpha\alpha} \sin 2\beta - K_{\beta\beta} \sin 2\alpha}{\cos\alpha \cos\beta \sin(\beta - \alpha)} \qquad 2.31$$

$$K_{vf} = \frac{1}{2} \frac{K_{\beta\beta} \cos^2\alpha - K_{\beta\beta} \cos^2\beta}{\cos\alpha \cos\beta \sin(\beta - \alpha)} \qquad 2.32$$

Putting Re and Im components of $K_{\alpha\alpha}$ and $K_{\beta\beta}$ of inner and outer modulation into equations (2.31, 2.32) instead of $K_{\alpha\alpha}$ and $K_{\beta\beta}$ gives:

$$\begin{array}{llll} Re(K_{ff})_i & Im(K_{ff})_i & Re(K_{ff})_o & Im(K_{ff})_o \\ Re(K_{vf})_i & Im(K_{vf})_i & Re(K_{vf})_o & Im(K_{vf})_o \end{array}$$

All above stiffnesses are related to the displacement in the feed direction, they can also be considered as force vector components respective along the v or f axes for unit displacement in the chip thickness modulation.

The angle of a force component with respect to f direction is given by:

$$tg\ \theta = \frac{K_{vf}}{K_{ff}} \qquad 2.33$$

And then, the direction angles are yielded from the four force vectors.

$$Re(F_i) \quad Im(F_i) \quad Re(F_o) \quad Im(F_o)$$

$Im(F_i)$ has the physical meaning of a damping. The method involves two test rigs and is very elaborate for execution. According to the presented results the "negative" damping was not experienced.

Kals(6) suggested in his work that the cutting process adds stiffness and damping to the total machining system over that available from the machine tool structure. Thus, he proposed the total machining system as shown in Fig. 4.1.

K and c represent stiffness and damping of the machine tool structure and k_p and c_p, the corresponding quantities due to the cutting process.

A single degree of freedom system was used, whose compliance in its model direction was much higher than that of the machine tool. The behaviour of inner modulation was studied. Using equation (3.9) it can be written on the limit of stability.

$$b_{lim}\, k_i = \frac{1}{2(-Rn)} \qquad 2.34$$

For a single degree of freedom system it can be derived:

$$R_n = -\frac{1}{k}\,\frac{1}{4\xi(1+\xi)} = -\frac{1}{2c\omega_o} \qquad 2.35$$

where k_i is the specific cutting process stiffness, k is the stiffness of the system, ξ is the damping ratio, ω_o is the natural frequency. And it follows:

$$b_{lim}k_i = c\omega_o \qquad 2.36$$

If, during cutting, a process damping c_p is added to the system equation 2.36 can be rewritten.

$$b_{lim}k_i = (c + c_p)\,\omega_o = c_c\omega_o \qquad 2.37$$

Exciting the tool by a pulse during cutting, it is possible to measure the displacement response before regeneration occurs. From this the damping ratio of the system is obtained

$$\delta = \frac{1}{n}\,\ln\frac{A_o}{A_n} \qquad 2.38$$

$$\delta \cong 2\pi\xi_c \qquad 2.39$$

where δ is logarithmic decrement, A_o/A_n is amplitude ratio, ξ_c is the damping ratio of the system during cutting. The damping ratio of the system can be written as

$$\xi_c = \frac{c_c}{2\sqrt{m(k + bk_i)}} \qquad 2.40$$

and consequently for damping of the system

$$c_c = 2\,\xi_c\sqrt{m(k + bki)} \qquad 2.41$$

Then on the threshold of stability the following relations are valid:

$$b_{lim}k_i = c_c\omega_o = 2\,\xi_c\sqrt{k(k + bki)} \qquad 2.42$$

$$b_{lim}k_i = 2k\,(\xi_c + \xi_c^{\,2} + \ldots.) \qquad 2.43$$

Neglecting second and higher orders and knowing $k = m\omega_o 2$ it can be written:

$$k_i = \frac{2m\omega_o 2\,\xi_c}{b_{lim}} \qquad 2.44$$

If the stability chart under certain conditions is known it is possible to calculate k_i with the aid of the ξ_c - values obtained from the logarithmic decrement. And knowing that:

$$\xi_c = \frac{\omega_o}{\omega_o} - 1 \qquad 2.45$$

Then equation (3.44) is rewritten as:

$$k_i = \frac{2m}{b_{lim}}\,\omega_o(\omega_c - \omega_o) \qquad 2.46$$

Tobias' equation (2.4) was used for expressing damping and was written as:

$$\Delta F_\alpha = b\left[(|\vec{k}_i|\cos\beta)\,\Delta h - (|\vec{c}_i|\cos\gamma)\Delta\left[\frac{dy}{dt}\right]\right] \qquad 2.47$$

where ΔF_α is a projection of the dynamic component of the resultant cutting force on the principal direction of motion, Δh is chip thickness modulation, β and are the angles between k_i and c_i and the principal direction of motion respectivelly, see Fig. 8.5. The overall damping ratio is written as:

$$\xi_c = \frac{c + b_{lim} c_i}{2\sqrt{m(k + b_{lim} k_i)}} \qquad 2.48$$

And for specific process damping the formula is:

$$c_i = \frac{2m}{b_{lim}} \left(\frac{\omega_c}{\omega_o} (\omega_c - \omega_o) - \xi \omega_o \right) \qquad 2.49$$

where ξ is the damping ratio of the system for b = 0.

Values k_i and c_i obtained this way are projections of the original vectorial quantities k_i and c_i. In the case orthogonal cutting k_i and c_i act in a plane through the direction of the normal cutting force F_n and tangential cutting force F_t. To determine both k_i and c_i two different testing rigs with different principal directions are needed. Fig. 8.5 shows diagramatically the composition of k_i and c_i. The method is very simple and it does not need complex test apparatus for performing.

Dautzenberg (18) used Kals' method for determinating the imaginary part of the direct inner DCFC, $\alpha = 0$. The experiments were conducted on the workpiece which was specially arranged, Fig. 2.4, to exclude the regeneration. The experiment was conducted with one workpiece material.

2.3 Other investigations on the dynamic cutting process

A number of researchers have attempted to study the dynamic cutting process using high speed photography. Basically they tried to develop theoretical models which could predict certain cutting conditions like shear angle variation. The already known static cutting data were then used to calculate the cutting forces.

Sarnicola and Boothroyd (19,20) studied the dynamic response of the shear angle in wave removing (22) and wave cutting and regeneration (23). The variation of shear angle was measured from the distortion of striations which were scribed perpendicular to the cutting direction on the side of the workpiece. The measurement of cutting forces was also undertaken. A theoretical model was formulated which predicted fairly accurately the dynamic force components in wave removing.

For wave cutting and regeneration experiments high speed photography technique was used. The effect of

the instantaneous work surface slope on the shear angle was studied. The variations in shear angle during wave generating and regenerative chatter situations were measured and compared with results of previous wave removing tests. An model for predicting the response of the shear angle was built.

Brass 90/10 was used as a workpiece material and the cutting speeds were extremely small (1-2 fpm).

Stewart and Brown (21) formulated a mathematical model which relates the coefficient of friction as a function of the instantaneous shear plane angle, instantaneous shear plane length and instantaneous rake angle. Force equilibrium is considered in the manner proposed by Merchant. This assumes that the resultant forces on the shear plane and rake face are equal, opposite and collinear.

A high-speed camera was used to record the instantaneous shear geometry in an orthogoual cut. Forces were measured by a two-component strain gauge dynomometer. Experiments reveals that the normal force is in phase with the shear plane length and that the frictional force is 180° out-of-phase with the normal force and the shear plane length.

Cold drawn steel 1010 was used as a workpiece material, the cutting speed was 730 ft/min.

Experimental results verified the formulated mathematical model. However the verification was limited to one steel, one feed rate and as mentioned above to one cutting speed.

CHAPTER III

SIMPLIFYING THE TASK OF MEASURING THE DCFCs

As stated in Chapter 1 different types of vibrations are experienced during machining of metals. Some of these vibrations are of minor importance, some of them, especially those generated in the cutting process and of self-excited nuture, have a great significance.

The development of predicting the stable machining and the simplification in using some of the DCFC as proposed by Tlusty are briefly presented in this chapter.

3.1 Principles of Self-excited Vibrations

The basic diagram of the process of self-excited vibrations in metal cutting was identified by Tlusty (8) and is shown in Fig. 3.1a), reproduced from (7).

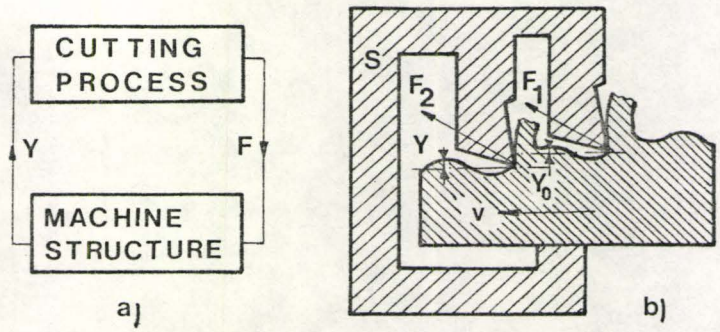

Figure 3.1 Basic diagram of chatter

It is a closed loop system having two fundamental parts: the cutting process and the vibratory system of the machine and the mutual directional orientation of the two parts. It indicates that the vibration Y between the tool and the workpiece influences the cutting process so as to cause a variation of the cutting force F which, acting on the vibratory system of the machine creates again vibration Y.

In experimental work it has been found that the stability of different types of machines can be related to one criterion and that is chip width. The cutting test is usually performed this way: it starts under standard cutting conditions (feed rate, cutting speed) with a small width b. By increasing b to such a point that chatter starts to occur the limit of the chip width b_{lim} is found. This kind of test can be performed for different cutting speeds and feeds as well. The value b_{lim} can be used as a criterion of stability. Fig. 3.2 shows the relationship between the b_{lim} and the cutting speed as it appears for most of workpiece materials.

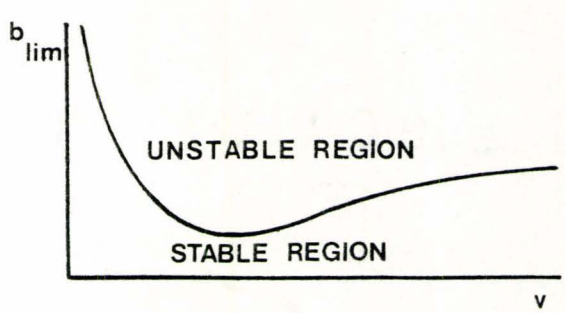

Figure 3.2 Effect of cutting speed on limit of stability.

According to Fig. 3.1a , the cutting process is represented by the transfer function relating vibration Y to force F. For small variations, see Fig. 3.3, reproduced from (1), the force-displacement transfer function is linearised. The average values of the chip thickness and of the force do not influence the vibratory process and the transferfunction is expressed as a relationship between variable components of the chip thickness and force:

$$F = R.Y \qquad 3.1$$

where the coefficient R expresses the intensity of the coupling between the vibration and the cutting force.

For usual chip thickness, Y is the normal to the main cutting edge and the coupling between Y and F is proportional to the chip width b. Equation 3.1 can be re-written.

$$F = b.r.Y \qquad 3.2$$

where the coefficient r depends on all cutting conditions but it does not depend on b.

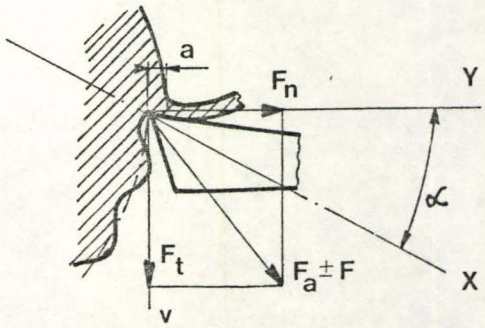

Figure 3.3. Changes of chip thickness produced by vibration Y.

The two most powerful principles of chatter were recognized by Tlusty. They are:

- the regenerative chatter
- mode coupling

The regeneration principle is based on the fact that, with the exception of artificially arranged cases, see Fig. 3.4, the tool always cuts a surface which has been already cut during the previous cut. It means the tool T_1 leaves an undulated surface with amplitude Y_o behind which being cut by the following tool T_2 (tooth in the case of milling cutter, or the following pass by the same tool in the case of turning) which leaves again an undulated surface behind with the amplitude Y, Fig. 3.1b.

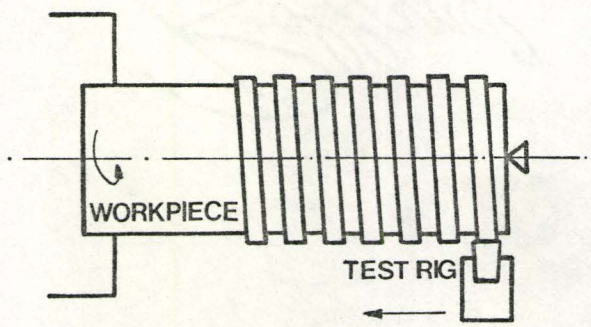

Figure 3.4 The non-regenerative set up

Assuming linear vibratory system of the machine and single tool, it can be written for the cutting force:

$$F = -b.r. (Y - Y_o) \qquad 3.3$$

where $Y - Y_o$ is undeformed chip thickness variation, b - chip width and r is the coefficient of proportionality or the cutting stiffness. The coefficient r is assumed to be a real number. In such a case variation of force depends on the chip thickness variation and no damping is generated in the chip formation process.

And for the absolute cross transferfunction of the vibratory system according to Fig. 3.1b, it can be written:

$$Y = F.\Phi(\omega) \qquad 3.4$$

where: $\Phi(w) = G(\omega) + jH(\omega)$

$$= \sum_{1}^{i=n} u_i G_i + j u_i H_i$$

G and H are its real and imaginary parts respectively and ui are the directional factors of individual modes in the case of multidegree of freedom system.

Equations 3.3 and 3.4 can be combined into:

$$\frac{Y}{\Phi} = b.r.\ (Y - Y_o) \qquad 3.5$$

and after rearranging:

$$\frac{Y_o}{Y} = \frac{1/b.r + \Phi}{\Phi} \qquad 3.6$$

On the limit of stability it is:

$$|Y_o| = |Y| \qquad 3.7$$

which means that the amplitude of vibration in cut Y is equal to the amplitude of Y_o and vibrations of the previous cut. And because of the assumption that r and b are real numbers, the limit of width is derived as:

$$b_{lim} = -\frac{1}{2r\ G_{min}} \qquad 3.8$$

or as it is used to write:

$$b_{lim} = -\frac{1}{2r\ Re(G)_{min}} \qquad 3.9$$

where G_{min} is the magnitude of the real part of the transferfunction of the structure oriented with respect to the direction of the cutting force and to the direction of the normal to the cut surface, see (1,2).

The second principle of self-excited vibration, "the mode coupling" can be only applied within the vibration system which has at least two degrees of freedom as presented in Fig. 3.5, reproduced from (1).

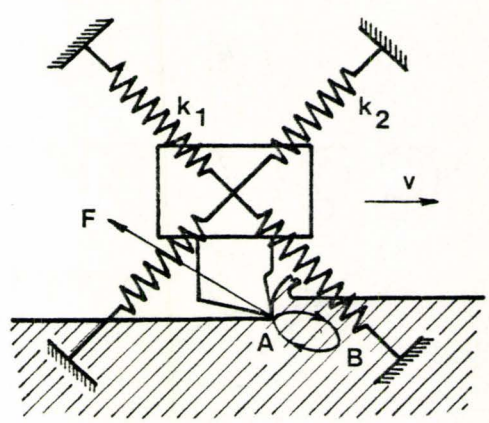

Figure 3.5 Mode coupling principle

This condition is always fulfilled in case of machine tool structures.

During machining under vibratory condition the tool describes an eclipse. During the motion A to B the cutting force acts against the motion. In this period energy is dissipated. During the motion B to A the cutting force acts in the direction of the velocity of the motion. Therefore energy is delivered to the system. Since during the second half of the cycle the tool faces a larger average depth of cut, the average force in this period is greater than in the first period. Thus, for each cycle an excess energy is available which may overcome the damping and maintains vibrations in the system.

3.1.1 The necessity of respecting damping generated in the cutting process

In the preceeding section the cutting process was characterized by a real coefficient r, the cutting stiffness. This coefficient changes with cutting speed or feed and workpiece material but not enough to explain the observed variation of b_{lim}. Looking on Fig. 3.2 it can be seen that very high values of b_{lim} occur in the low range of cutting speed, low values in the middle range and increasing values of b_{lim} for higher speeds.

From this behaviour a conclusion can be drawn. Not only a stiffness but also damping - positive and negative - is included in the cutting process and it has a rather strong effect on stability of cutting. The coefficient r as a real number could not fully express properties of the cutting process and was replaced by a complex coefficient known in metal cutting as the Dynamic Cutting Force Coefficient (DCFC).

3.2 The DCFC and limit of stability

In practical situations, as it is shown in Fig. 3.6 which was reproduced from (7) the vibrating tool removes the chip from the undulated surface with an amplitude Y_o of the previous cut and leaves behind a new undulation with an amplitude Y.

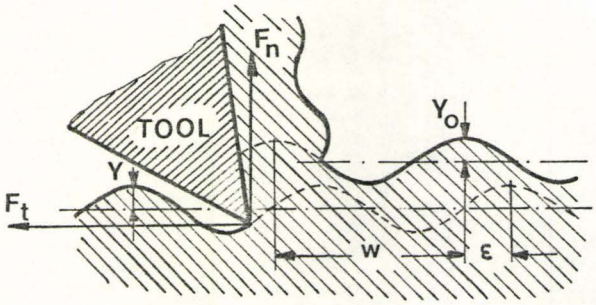

Figure 3.6 Regeneration of vibrations

The two components of cutting force - the normal force F_n and tangential force F_t - are dependent on the outer modulation Yo and on the inner modulation Y

because it is actually the difference between the two undulations which determines the instantaneous chip thickness which however, depends on the magnitudes Y_o and Y as well as on their mutual phase. This phase shift is included in the complex amplitudes and at the limit of stability it is:

$$\left| Y \right| = \left| Y_o \right| \text{ and } Y = Y_o e^{j\varepsilon} \qquad 3.10$$

The phase angle is either free to adjust itself for maximum regeneration or is constrained by the relationship between the frequency of vibration f, cutting speed v, and the length of cut between subsequent passes ℓ.

$w = \frac{v}{f}$ - the wavelength

$\frac{\ell}{w} = N + P$ where N is an integer such that $P<1$

$\varepsilon = 360\ P$ degrees

According to equations (3.1, 3.2) the transfer-function of the cutting process with regeneration can be written as:

$$F_n = b\ (K_{di}Y + K_{do}Y_o) \qquad 3.11$$

$$F_t = b\ (K_{ci}Y + K_{co}Y_o)$$

Both force components depend on the vibration in the direction of the normal Y only. The subscript d

means direct, being the effect of the vibration in the normal on the normal force. The subscript c means cross, being the effect of the vibration in the normal on the tangential force. The subscript i means inner and o means outer in regard to modulations.

Each of the four Dynamic Cutting Force Coefficients, K_{ij} in equation (3.11), is considered complex. Thus we deal with eight DCFC's.

$$K_{ij} = Re(K_{ij}) + {}_{j}Im(K_{ij}) \qquad 3.12$$

The real components determine forces in - phase with displacements causing them and they represent the "stiffness" of the spring - type relationship between the displacements and forces.

The imaginary components determine forces out - of phase with the displacements causing them and they represent "damping" generated in the cutting process.

The transferfunction of the machine tool structure can be written as:

$$Y = G_d F_n + G_c F_t \qquad 3.13$$

As it is known, Y is the relative vibration between the tool and the workpiece in the normal direction to the cut surface.

Imposing condition, equation (3.10), and combining equations (3.11) and (3.13), the expression for b_{lim} is obtained:

$$b_{lim} = \frac{1}{G_d\left[-K_{di} + K_{do}e^{\varepsilon}\right] + G_c\left[-K_{ci} + K_{co}e^{\varepsilon}\right]} \qquad 3.14$$

A single degree of freedom system can be assumed with direction of freedom X. This direction X is inclined by an angle α to the direction Y of the normal to the cut. $G(\omega)$ is the transferfunction of the system in the direction X, Fig. 3.3. Then it can be written:

$$G_d = G\cos^2\alpha \qquad 3.15$$

$$G_c = G\sin\alpha\cos\alpha$$

The directional factors are: $u_d = \cos^2\alpha$, $u_c = \sin\alpha\cos\alpha$

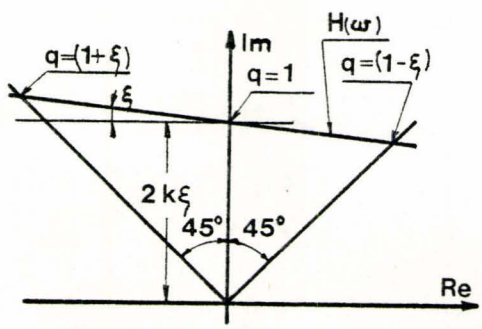

Figure 3.7 Single degree of freedom with direction X

Equation (3.14) becomes:

$$b_{lim} = \frac{1}{G\left[-u_d K_{di} - u_c K_{ci} + e^{\varepsilon}\left(u_d K_{do} + u_c K_{co}\right)\right]} \qquad 3.16$$

or

$$-u_d K_{di} - u_c K_{ci} + e^{\varepsilon}\left(u_d K_{do} + u_c K_{co}\right) = \frac{1}{b_{lim} G} \qquad 3.17$$

A case with $\alpha = 0$ is analysed first in which $u_d = u_c = 0.5$:

$$- K_{di} - K_{ci} + e^{\varepsilon}\left(K_{do} + K_{co}\right) = \frac{1}{0.5\, b_{lim} G} \qquad 3.18$$

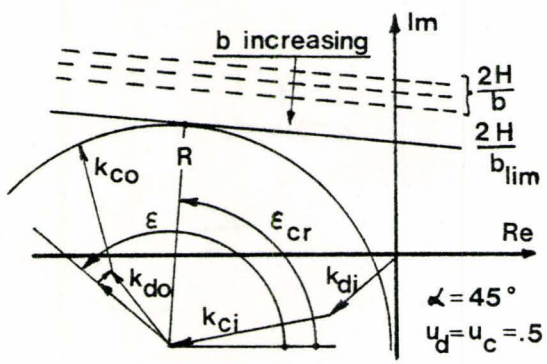

Figure 3.8 Limit of stability of single-degree of freedom

Denoting $H = \frac{1}{G}$ The function H is expressed as:

$$H = k\left[1 - \left(\frac{\omega}{\omega_n}\right)^2 + 2j\xi\frac{\omega}{\omega_n}\right] \qquad 3..19$$

or

$$H = k\left[1 - q^2 + 2j\xi q\right] \qquad 3.20$$

where k is the stiffness, ω is an angular frequency and ω_n is the natural frequency and ξ is a damping ratio of the

system. Fig. 3.7, reproduced from (7), shows function H expressed graphically. Equation (3.18) can be rewritten as:

$$- K_{di} - K_{ci} + e^{\varepsilon} (K_{do} + K_{co}) = \frac{2H}{b_{lim}} \qquad 3.21$$

In Fig. 3.8, reproduced from (7), equation (3.21) is explained. The complex inner coefficients K_{di} and K_{ci} are added in point S. For arbitrary ε a circle is drawn with $R = K_{do} + K_{co}$. A line $\frac{2H}{b}$ is inclined by ε with respect to the real axis. With increased values of b the line moves downwards. Finally it touches the circle and b_{lim} is reached. On Fig. 3.8 the influence of individual DCFC's on b_{lim} can be drawn:

- the real part of the inner coefficient does not have any practical effect on b_{lim}
- the imaginary direct and cross coefficients and are the most influential
- b_{lim} is almost in an inverse proportion to:

$$\left| K_{co} + K_{do} \right| - Im(K_{di}) - Im(K_{ci})$$

For angle $\alpha \neq 45^{\circ}$ it can be written:

$$\frac{1}{2k_{\eta}} \left\{ \left| u_c K_{co} + u_d K_{do} \right| - u_d Im(K_{di}) - u_c Im(K_{ci}) \right\} \cong \frac{1}{b_{lim}} \qquad 3.22$$

From experimental results (4,5,9,10,11,12) another simplification can be made. The imaginary part of outer coefficients are very small and can be neglected. Then, equation (3.22) becomes:

$$\frac{1}{2k\xi_1}\left\{u_c Re(K_{co}) + u_d Re(K_{do}) - u_d Im(K_{di}) - u_c Im(K_{ci})\right\} \cong \frac{1}{b_{lim}} \qquad 3.23$$

and it can be assumed that real parts of outer and inner coefficients are equal. This was confirmed by experiments as well.

$$Re(K_{do}) + Re(K_{co}) = Re(K_{di}) + Re(K_{ci}) \qquad 3.24$$

Then equation (3.23 with $\alpha = 45^o$ ($u_d = u_c = 0.5$) and equation (3.24), can be expressed graphically as shown in Fig. 3.9, reproduced from (7)

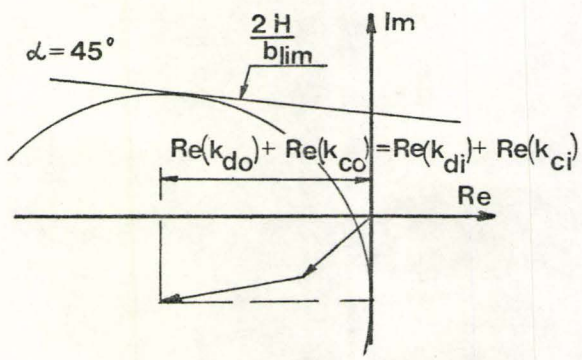

Figure 3.9 Limit of stability with imposing equation (3.24)

For $\alpha = 0$ ($u_d = 1$, $u_c = 0$), equation (3.23) becomes:

$$\frac{1}{2k\xi_1}\left\{Re(K_{do}) - Im(K_{di})\right\} = \frac{1}{b_{lim}} \qquad 3.25$$

and using the above assumption, equation (3.24), equation (3.25) can be rewritten as:

$$\frac{1}{2k_{di}}\left\{Re(K_{di}) - Im(K_{di})\right\} = \frac{1}{b_{lim}} \qquad 3.26$$

Graphically, equation (3.26) is presented in Fig. 3.10 which is reproduced from (7)

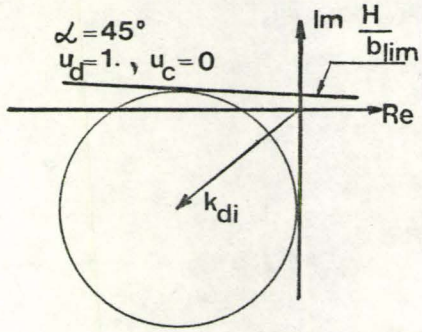

Figure 3.10 Limit of stability for a mode in direction Y

Examining equation (3.22), for cases when $\alpha \neq 0^{o}$ or 45°, it may be concluded:

- the larger $\left|u_c K_{co} + u_d K_{do}\right|$ is the smaller is b_{lim}
- the damping $\left[u_d Im(K_{di}) + u_c Im(K_{ci})\right]$ can be positive or negative and it correspondingly affects b_{lim}

The conclusion from the examination of equation (3.26), for a case when $\alpha = 0$, may be written as:

- if $Re(K_{di}) = Im(K_{di})$ infinitive stability is obtained.

3.3 Conclusions

The complexity of the DCFC's was the main obstacle in developing a method which would produce reliable data. The approaches employed by different laboratories were presented in Chapter 2. Usually all eight components of the DCFC have been tried to obtain. As it is seen in (7) rather large discrepancies were found.

The analysis (7), presented in section 3.2, simplifies the approach to the complex problem of the DCFC's. If the assumption of equation (3.24), that real parts of outer and inner coefficients are equal, is imposed in equation (3.23), then it can be rewritten as:

$$\frac{1}{2k_1}\left\{u_c \mathrm{Re}(K_{ci}) + u_d \mathrm{Re}(K_{di}) - u_d \mathrm{Im}(K_{di}) - u_c \mathrm{Im}(K_{ci})\right\} \cong \frac{1}{b_{lim}} \qquad 3.27$$

To solve equation (3.27) a method is needed for measuring the real and imaginary direct and cross coefficients of the inner modulation only.

The measurements of the direct and cross coefficients can be performed separately. It can be done by using two test rigs. One rig which has the 2nd principal direction of motion, $\alpha = 0$, for measuring the direct coefficients. The second rig with the 1st principal direction of motion, $\alpha \neq 0$, for measuring the cross coefficients.

CHAPTER IV

THEORETICAL BACKGROUND AND DEVELOPMENT OF EXPERIMENTAL TECHNIQUE

Considerable research efforts have already been devoted to investigations of the Dynamic Cutting Force Coefficients. Most of the experiments were carried out at steady constant amplitude of vibration of the tool by means of an exciter and with the measurement of force and vibration components. Usually these tests were done under regenerative conditions, i.e. with the simultaneous action of the outer and inner modulations. This aspect increases the complexity of the test arrangement. It is necessary to synchronize the vibration with spindle revolutions and double the set-up so, as to separate the two effects. Moreover, the regeneration itself may lead to self-excited vibrations and therefore the test has to be done with rather stiff rigs and then the dynamics of the machine tool used is not negligible.

It is known from Chapter 3 that the $Im(K_{di})$, the imaginary direct inner modulation DCFC, is the most significant and represents the positive or negative damping in the cutting process.

The present work reviews and modifies one of the simplest methods suggested by Kals (6). Only measurement of vibrations of inner modulation is carried out, which means regeneration is excluded. The interest is especialy in the transient vibration produced by an impact.

4.1 Theoretical development

Starting with the single degree of freedom system, Kals' assumption that the cutting process adds stiffness and damping to the equivalent quantities of the structure is taken over. The model is represented in Fig. 4.1.

With respect to what is said above about the non-significance of the outer modulation, the first suggestion for simplification is:

- to test under non-regenerative conditions (Fig. 2.4)

and the others:

- the orientation of the principal direction of the motion of the structure is perpendicular to the surface cut
- neglecting of the mode coupling

The orthogonal cutting is applied to reduce the geometric

problem to a plain one.

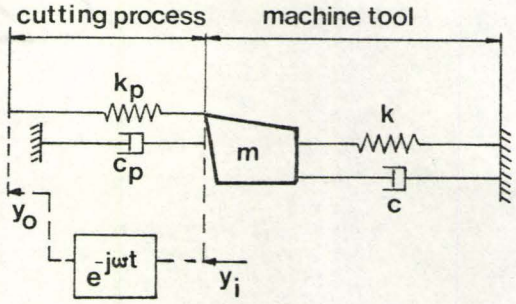

Figure 4.1 Model on cutting dynamics (after Kals)

Being k_c the overall stiffness and c_c the overall damping coefficient during cutting and y the direct chip thickness modulation, Fo - the dynamic component of cutting force, ω_c - cutting frequency. Then the differential equation of motion can be written as:

$$m\frac{d^2y}{dt^2} + c_c\frac{dy}{dt} + k_c y = Fo \sin \omega_c t \qquad 4.1$$

or

$$m\frac{d^2y}{dt^2} + (c + c_p)\frac{dy}{dt} + (k + k_p)y = Fo \sin \omega_c t \qquad 4.2$$

where m is mass of the test rig, c is the damping coefficient of the system before cutting and k is the stiffness of the system before cutting (respective cutting with b = O, b - width of cut). C_p and k_p are quantities added by cutting process, they can be called the process damping coefficient and the process stiffness respectively. And

in fact they represent the imaginary and real components of DCFC for inner modulation. The process stiffness can be expressed as:

$$k_p = k_c - k = m\omega_c^2 - m\omega^2 = m\omega^2 \left(\frac{\omega_c^2}{\omega^2} - 1\right) = k \left(\frac{\omega_c^2}{\omega^2} - 1\right) \qquad 4.3$$

and the process damping coefficient:

$$c_p = c_c - c = 2\xi_c m\omega_c - 2\xi m\omega = 2m\,(\omega_c\xi_c - \omega\xi) \qquad 4.4$$

knowing:

$$c = \xi\, c_{cr} = \xi\, 2\sqrt{km} = 2\xi m\omega$$

As it is seen in equation (4.3) the $Re(K_{di})$ is obtained with less sensitivity from the change of the frequency and with relating to the width of cut b:

$$Re(K_{di}) = \frac{kp}{b} \qquad 4.5$$

The damping force is $F_d = c_p A\omega_c$, where A is the amplitude of vibration. The value of $Im(K_{di})$ according to equation (2.11) is related to the width of cut b and to the amplitude:

$$Im(K_{di}) = \frac{F_d}{bA} = \frac{c_p}{b}\,\omega_c \qquad 4.6$$

In all this the effect of damping on frequency was neglected.

4.2 Processing and evaluating the signal

To evaluate the process stiffness k_p and the process damping coefficient c_p four quantities are needed to be measured, see equations (4.3, 4.4). These quantities are:

ω-frequency of the rig when the width of cut b = 0, idling (natural frequency of the rig, the effect of damping is neglected)

ω_c-frequency of the rig during cutting, b = 2.5 mm

ξ-damping ratio of the rig when the width of cut b = 0

ξ_c-damping ratio during cutting, b = 2.5 mm

The mass m of the rig is a known quantity and is constant during whole test. In practice, ω, ω_c ξ and ξ_c are obtained by evaluating the records of transient vibrations produced by an impact. The frequencies and ω_c are simply counted. The damping ratios ξ and ξ_c are evaluated visually by fitting the signal to templates corresponding to various decay rates, see Figs. 8.7, 8.8, 8.9, 8.10. The vibration signal decays as:

$$x = Xe^{-\lambda t}(\sin \omega t + \phi) \qquad 4.7$$

$$\xi = \frac{\lambda}{\omega} \qquad 4.8$$

where X is vibration of the mass in the direction denoted (x), λ is the logarithmic decrement, ω is the vibration frequency and ϕ is the phase angle.

Each computed point of the DCFCs on the graphs, see Figs. 8.12, 8.13,...., is the average of four sets of data which consist of four measured quantities as mentioned above. The reliability of the measurements was cross checked by setting different damping ratios of the test rig as described in section 6.3.

4.3 Differences between Kals' method and the new method

Kals' main contribution is the idea to obtain the damping of the cutting process by comparing transient vibrations of a test rig in the cut with that outside of the cut, see [5]. This provides a very straightforward assessment of the damping in the cutting process. However, his overall arrangement of the test was not very advantageous and his practical results, especially in the low cutting speed range were rather poor.

He set up his experiment so as to test at the limit of stability. In this way he had to cope with a mixture of two influences: regeneration of waviness and damping in the cut. He also had to use a rather stiff

test rig. Otherwise he would have obtained strong excitation. The stiff rig is then not removed far from the modes of the lathe used and cannot be considered purely single degree of freedom. The effect of changes of the damping in the cut on the decay of the transient vibration of a stiff rig was necessarily small and, therefore, not easily measurable.

Furthermore, the actual design of the rig consisting of several parts bolted together provided a rather high damping ratio of the rig itself ($\zeta = 0.08$) which, again, overshadowed the effects of the damping in the cut. Also, the damping of the rig depended on the feed velocity as it affected the state of the gap in the guideways.

In the new method regeneration of waviness is completely excluded by means of an arrangement as described in relation to Fig. (3.4). The decay rates of the transient vibrations cannot, therefore, be influenced by any self-excitation and they are subject solely to the influence of the damping in the cutting process. It is, therefore, also possible to use a rather flexible rig which is very sensitive to the damping in the cut.

The design of the rig is such that it was milled out of one piece minimizing the number of joint surfaces. This resulted in a very low damping ratio of the rig itself ($\xi = 0.005$) and when mounted on the lathe ($\xi = 0.012$) which further increased the sensitivity to variations of the damping in the cut.

Perhaps the most important feature of the new method is the capability of varying the damping of the rig itself so as to obtain easily interpretable decay rates both for low and high damping in the cut. This controllability of the damping of the rig is achieved by using a very low mechanical damping as mentioned above in combination with a controllable additional electrically generated damping. The latter is rather strongly linear being based on electrodynamic excitation.

All these substantial improvements of the original test method of Kals led to a qualitatively new situation permitting a high level of sensitivity and of distinction of even slight variations in the cutting process damping.

CHAPTER V

EXPERIMENTAL EQUIPMENT

The experimental equipment for the method was developed to meet the requirements and conditions needed for the evaluation of the Dynamic Cutting Force Coefficients in accordance with theoretical conditions outlined in Chapters 3 and 4.

5.1 General description

The experimental set-up for the measurement of the DCFC's is shown in Fig. 8.6a). Fig. 8.11b) shows the actual photograph of the equipment.

On the test rig, Fig. 8.6a) and 8.11b), a capacitive probe for measuring the tool displacement is mounted. The signal is fed into the Wayne Kerr bridge to obtain an equivalent voltage signal. This signal goes one way to the recorder and another way to a phase shift circuit, Fig. 8.6b). The shifted signal, $+90^{\circ}$, has to be amplified by means of the power amplifier and fed into the coil of the electrodynamic exciter which is a part of the rig.

The function of the power amplifier is to vary the voltage of the shifted signal and in such a way to vary the damping ratio of the rig from 0.012 to 0.09 level (the rig is damped).

By means of changing the polarity (after amplifying) the signal is shifted 270°. This means that the negative damping is introduced to the rig. Lower values of the damping than 0.012 are reached.

The purpose of varying of the damping ratio of the rig is in adjusting the damping for a reasonably well decay rate at various cutting conditions as described in section 6.3.

The experimental set-up consists of:

- the test rig
- the capacitive probe MDI-513
- the phase shift circuit
- Wayne Kerr bridge B731 B
- Power amplifier 2250 MB
- Honeywell 2206 visicorder

The experiments were conducted on the TOS SN 40-B lathe.

5.2 Test rig.

The test rig was designed as a single degree of freedom system, see Fig. 8.6a) and 8.11b). The orientation of the principal direction of the motion is in the direction of the chip thickness modulation, α - 0°.

The rig consists of mass m=4.82 kg on two vertical parallel flat springs at the ends. The main body of the rig is produced in one piece to avoid any dependency of the rig damping on the preload produced by the cut if springs were attached by bolts.

The natural frequency of the rig is 200Hz, the dynamic stiffness of the rig is 7.61×10^3 N/mm. The damping ratio of the rig is 0.012 when mounted on the lathe. As stated in section 4.3, alone it has still smaller damping ratio of about 0.005 but the reactions to its vibrations in the guide ways of the slide increase its damping but to a still well tolerable level. The damping ratio of the rig was checked before each test and has stayed on the 0.012 level.

On the one end of the rig an electrodynamic exciter is attached. The maximum power is 100W.

5.3 Phase shift circuit.

Fig. 8.6b represents the diagram of the phase shift circuit.

The function of the circuit is to shift the signal from the capacitive probe by 90° and this introduces damping to the system at the natural frequency of the rig.

System of the low pass filter and high pass filter was used, see Fig. 2.7a.

Denoting:

$$Z_1 = \frac{1}{j\omega C_1} = \frac{1}{sC_1} \qquad 5.1$$

$$Z_2 = R_1 \qquad 5.2$$

$$Z_3 = R_2 \qquad 5.3$$

$$Z_4 = \frac{1}{j\omega C_2} = \frac{1}{sC_2} \qquad 5.4$$

The output voltages can be determined as:

$$v_a = \frac{Z_2}{Z_1 + Z_2} v_i \qquad 5.5$$

$$v_o = \frac{Z_4}{Z_3 + Z_4} v_a \qquad 5.6$$

$$v_o = \frac{Z_4}{Z_3 + Z_4} \times \frac{Z_2}{Z_1 + Z_2} v_i \qquad 5.7$$

The transferfunction of the circuit can be written as:

$$\frac{v_o}{V_i} = \frac{R_1}{C_2 s} \frac{1}{\left(\frac{R_2}{C_1 s} + R_1 R_2 + \frac{1}{C_1 C_2 s^2} + \frac{R_1}{C_2 s}\right)} \qquad 5.8$$

Denoting: $C = C_1 C_2$, $R = R_1 R_2$

It can be derived:

$$\frac{v_o}{v_i} = \frac{C_1R_1\ s}{CRs^2 + (C_2R_2 + \frac{R_1C}{C_2})s + 1} \qquad 5.9$$

The numerator can be expressed in a general form as:

$$1 + \tau j\omega \qquad 5.10$$

It represents the first - order system. Bode diagram for this simple lead is shown in Fig. 8.7b. The phase angle is given by:

$$\phi_1 = -\tan^{-1}\tau\omega \qquad 5.11$$

τ - is the time constant

When $\tau\omega$ approaches ∞ 90° phase shift is reached.

The denominator can be expressed in a general form as:

$$\frac{1}{(\lambda j\omega)^2 + 2\xi\lambda(j\omega) + 1} \qquad 5.12$$

and represents in the transferfunction a quadratic lag.

Where $\lambda = \frac{1}{\omega_n}$, ξ is damping ratio of the system.

Bode diagram for a quadratic lag is shown in Fig. 8.7c. The phase angle is given by:

$$\phi_2 = -\tan^{-1}\frac{2\xi\omega\lambda}{1-(\omega\lambda)^2} \qquad 5.13$$

At low frequency ϕ approaches 0°, when $\lambda\omega \gg 1$ ϕ approaches -180°.

By combining the two systems, the desired phase shift 90° can be reached.

$$\phi = \phi_1 + \phi_2 \qquad 5.14$$

Denoting:

$$\lambda^2 = CR = C_1C_2R_1R_2$$

$$\lambda = \sqrt{C_1C_2R_1R_2}$$

It can be written:

$$2\xi\lambda = C_2R_2 = \frac{R_1C}{C_2}$$

$$= C_2R_2 + R_1C_1 \qquad 5.15$$

$$\phi_1 = \tan^{-1}(C_1R_1\omega) \qquad 5.16$$

$$\phi_2 = \tan^{-1}\frac{(R_1C_1 + R_2C_2)\omega}{1-C_1C_2R_1R_2\omega^2}$$

When: $C_1 = C_2 = .22\mu F$

$R_1 = 10\ M\Omega$

$R_2 = 37\ k\Omega$

$\phi = \phi_1 + \phi_2 =$

$= 89.98 - 174.40 = -84.42^\circ$

CHAPTER VI

RESULTS AND DISCUSSIONS

Series of tests were executed in which the Dynamic Cutting Force Coefficients were measured. The tests were conducted for three materials under various cutting conditions. The results and discussions are presented in accordance with the main objectives of this work outlined in Chapter I.

6.1 Workpiece preparation and materials

As it has been described in Chapter 4, the test has to be carried out in non-regenerative condition, Fig. 2.4. To fulfil this condition a stiff cylindrical workpiece is clamped between chuck and center and a flat thread is pre-cut on its surface. The specification of the thread:

width of the thread - 2.5 mm

pitch of the thread - 5 mm

Diameter of the workpiece: 100 mm

The DCFC's were measured for two steel materials 1045 and 4340 and for Al alloy 7075. The properties of these materials are given in Table 6.1

TABLE 6.1

Workpiece Material	Brinell Hardness (B.H.N)	Yield Strength (P.S.I)	Chemical Composition %							
			C	Mn	P	S	Si	Ni	Cr	Mo
1045 steel	170	54,250	0.45	0.70	0.04	0.05				
4340	270	68,500	0.40	0.75	0.04	0.04	0.275	1.82	0.80	0.25
			Zn	Mg	Cu	Cr				
7075 Al alloy	60	15,000	5.5	2.5	1.5	0.3				

6.2 Cutting tools and cutting conditions

The cutting tools used are described below:

HSS - Capital 395

Rake angle $\alpha = 7^{o}$

Clearance angle $\gamma = 7^{o}$

Sintered Carbide - Kenametal K420

Rake angle $\alpha = 7^{o}$

Clearance angle $\gamma = 7^{o}$

The cutting conditions for 1045 and 4340 materials:

Cutting Speed	- 15÷45 m/min	- using HSS tool
	- 45÷200m/min	- using K420 insert
Mean chip thickness	- 0.20 mm	
Flank Wear	- 0.00 mm	
(V_B)	- 0.15 mm	
	- 0.25 mm	

The cutting conditions for 7075 material:

Cutting Speed	-100÷800 m/min	- using K420 insert
Mean chip thickness	- 0.2 mm	
Flank Wear	- 0.00 mm	
(V_B)	- 0.25 mm	

The width of cut for all materials: 2.5 mm

6.3 Example of measured data

Fig. 8.8, 8.9, 8.10 present one series of tests made with 1045 material for these conditions:

- cutting speed	15 ÷ 180 m/min
- mean chip thickness (h_m)	0.2 mm
- flank wear (V_B)	0.0 mm

Natural frequency of the rig: 200 Hz

The tests at speeds v = 15 m/min to v = 46 m/min were made without any additional damping of the rig. The decay curve of the rig alone is given in Fig. 8.8a). It shows a damping ratio ζ = 0.012. In cutting v = 15 m/min the damping ratios are 0.10 and 0.105, see Fig. 8.8b). As the cutting speed increases the damping ratio is decreasing, down to 0.04 - 0.055 at v = 45 m/min, see Figs. 8.8c) to 8.8e).

When the cutting speed was increased to v=64 m/min (213 ft/min) vibration in the cut did not decay any more but increased, see Fig. 8.9a). This shows that at this speed there is negative damping in the cutting process which overcomes the 0.012 damping ratio of the rig.

Therefore, the damping of the rig was artificially increased to = 0.025, see Fig. 8.9b). Next to this record are the records 8.9b1), 8.9b2) made during cutting with this damping of the rig. Again, cutting is almost at the limit of stability.

Therefore, the damping of the rig was further increased to $\zeta = 0.025$ and the corresponding record without cutting is shown in 8.9c) and during cutting in 8.9c).

In Fig. 8.10 records are reproduced for still higher cutting speeds v=90, 126, 180 m/min (300,420,600 ft/min). In each of these cases it was necessary to use additional damping of the rig. The decay curves without cutting are given at the left in each a), b), c), d). To the right of them are the records obtained during cutting.

These presented methods for 1045 material reproduced from (22), show the way of conducting the experiments. The other tests were conducted in similar way for different conditions and materials outlined in sections 6.1 and 6.2

6.4 Discussions

The measured DCFC's are shown in Fig. 8.12 to Fig. 8.21. The Re (K_{di}) and Im (K_{di}) are plotted versus

Figs. 8.13 and 8.17 show the influence of the increased flank wear on the DCFC's. The flank wear was artificially done, V_B = 0.15 mm.

No big differences in values of Re (K_{di}) were experienced when compared with relevant values of Re (K_{di}) in Figs. 8.12 and 8.16.

In regard to the Im (K_{di}) values it can be said that there was a shift upward. It means that more positive damping is generated when cutting with a worn tool.

The shift was significant especially in the middle range of cutting speed. With material 1045 no negative damping was experienced, with material 4340 only very small values of negative damping were measured.

Figs. 8.14 and 8.18 show results obtained with a rather large flank wear, V_B = 0.25 mm.

Again an additional shift upward of the Im (K_{di}) coefficients of both materials was experienced. In the middle range of cutting speed no negative damping was measured.

cutting speed and the relevant materials and cutting conditions are shown on each graph. As it was said in section 4.2 the plotted points of the DCFC's are average values obtained from four measurements. The scatter of these values was found to be consistently small, especially for imaginary coefficients. Polynominal curves fitted to each of data sets are drawn.

6.4.1 DCFC's of 1045 and 4340 materials

Figs. 8.12 and 8.16 represent measurements of both materials when cutting was done with a sharp tool, the flank wear V_B = 0.0 mm

As it was discussed in (22), the method is more suitable for evaluating the damping generated in cutting process. Nevertheless the average value and general trend of the Re (K_{di}) agree with previous measurements, see (6).

The variation of Im (K_{di}) with cutting speed agrees well with the general experience: large positive damping at low cutting speeds, low and even negative damping in the region 40 - 120 m/min and low positive damping with little variation above 120 m/min. These results are in extremely good agreement with reliable previous results, see (6) and (9).

In regard to the Re (K_{di}) coefficients a downward trend was experienced, especially in the small and middle ranges of cutting speed. It means that lower values of the process stiffness were generated by cutting process.

Figs. 8.15 and 8.19 show the influence of the flank wear on the cutting frequency. With a rather small flank wear, V_B = 0.15 mm no changes in the cutting frequency are observed if compared with cutting frequency when V_B = 0.000 mm. But with the increased flank wear, V_B = 0.25 mm, the cutting frequency goes a little downward. This shift of cutting frequency is actually responsible in getting lower values of the process stiffness, see equation (4.3).

6.4.1.1 Influence of flank wear on process stiffness

The static tests were arranged to confirm the conclusion from section 6.4.1 that the process stiffness depends on the tool wear.

The incremental static stiffness k_i is expressed as the ratio of incremental cutting force ΔF to the increment in the depth of cut Δh for the normal and tangential cutting forces, see Fig. 8.1. Angle β represents the angle between the vector ΔF and the direction of motion of the tool.

It can be written:

$$k_i = k_{st} \cos \beta \qquad 6.1$$

$$k_{st} = \frac{\Delta F}{\Delta h} \qquad 6.2$$

The tests were conducted for the tool with flank wear V_B = 00 mm and the tool with V_B = 0.25 mm in the orthogonal cutting. The width of cut was 2.5 mm, the depth of cut h, = 0.2 mm and the increment Δh = 0.2 mm. Only F_v, the tangential force, was measured using the one component dynamometer for two cutting speeds:

27m/min $\Delta F_v = F_{v2} - F_{v1} = 541.1 - 332.1 = 209$ N (V_B = 0.00mm)

$\Delta F_v = 563.4 - 422.2 = 141.2$ N (V_B = 0.25mm)

40m/min $\Delta F_v = 518.9 - 311.3 = 207.6$ N (V_B = 0.00mm)

$\Delta F_v = 563.4 - 378.1 = 185.3$ N (V_B = 0.25mm)

where F_{v1} is related to h_1 and F_{v2} is related to h_2.

The static stiffness k_{st} cannot be computed because of having only the tangential forces. However, the results show that the incremental cutting force ΔF for the sharp tool is higher is compared with the incremental force for the warm tool. And it means that the final product, the incremental static stiffness, is higher for a sharp tool.

6.4.1.2 Influence of flank wear on process damping

The effect of the flank wear on the process damping can be explained by using Kegg's idea about the effect of flank interference on static forces. The measurements were done with a moderately worn tool, see Fig. 8.20, because it is the effect of the vibratory motion of the tool on forces F_n and F_t which is being considered it may be assumed that the top surface of the workpiece is flat see Fig. 8.20a). Both forces consist of a part which is proportional to the instantaneous chip thickness as shown in Fig. 8.20b) and of a part which depends on the interference of the tool flank, see Fig. 8.20c). The component in b, has an average value on which a harmonic component is superimposed in phase with the displacement Y_1. The component shown in c, would have a maximum when the tool is in position B and there is maximum flank interference. In this way this component is $\pi/2$ out of phase with motion y_1 and therefore it may constitute damping.

6.4.2 DCFC's of 7075 material

Fig. 8.21 represents measurements of DCFC's with a sharp tool, V_B = 0.0 mm. As it is seen on the figure the changes of Re (K_{di}) and Im (K_{di}) are only in the region 100 - 200 m/min. In the region 200 - 800 m/min both Re (K_{di}) and Im (K_{di}) keep the same values.

Fig. 8.22 shows measurements of DCFC's with a worn tool, V_B = 0.25 mm. The values of the process stiffness stayed on the same level during a whole test. Figure shows the small increase in the cutting frequency which was responsible for the increase of the process stiffness if compared to the process stiffness generated with a sharp tool.

The increase of the process damping was significant, especially in the speed range 100 - 400 m/min. In the range 400 - 800 m/min both coefficients kept the same level.

CHAPTER VII

CONCLUSIONS

This chapter briefly deals with the objectives which were laid out in Chapter I. Future areas of the work and unanswered questions are also indentified.

In regard to the first objective:

A new method was developed for measuring the Dynamic Cutting Force Coefficients of inner modulation. The method is based on the Kals' method. Section 4.3 fully describes the differences between the original Kals' method and the new method and shows the advantages of the new method.

The experimental results obtained with the new method are more convincing than any other experiments conducted so far in other laboratories and they represent a significant contribution to an extremely difficult experimental task.

The generated data represent the direct inner coefficients and the validity of these DCFC's could not be checked by comparing the experimentaly obtained b_{lim} with the theoreticaly computed b_{lim}, see section 3.3, because of the lack of the cross inner coefficients. However, a very

high level of repeatability, better than 20% - especially for the imaginery coefficients, and a good quantive and qualitative agreement between the new data and previous reliable data entitle the validity of the new method, see Figs. 8.24 and 8.25.

In regard to the second objective:

The measurements of DCFC's for three materials, 1045, 4340 and 7075, were carried out in accordance with the objective.

The effects of cutting speed and of the tool wear on the process stiffness and the process damping were studied as well.

In regard to future work:

It is recommended to build the second test rig for measuring the cross coefficients as mentioned in section 3.3.

Effects of the chip thickness (feed rate), tool geometry on the process stiffness and process damping should be investigated.

Also it is recommended to investigate the influence of the rig frequency on the process damping.

More efforts should be devoted in measuring of the DCFC's of non-ferrous metals.

These studies will enable us to get better knowledge about the DCFC's and predict the stable machining with better accuracy.

CHAPTER VIII

ILLUSTRATIONS

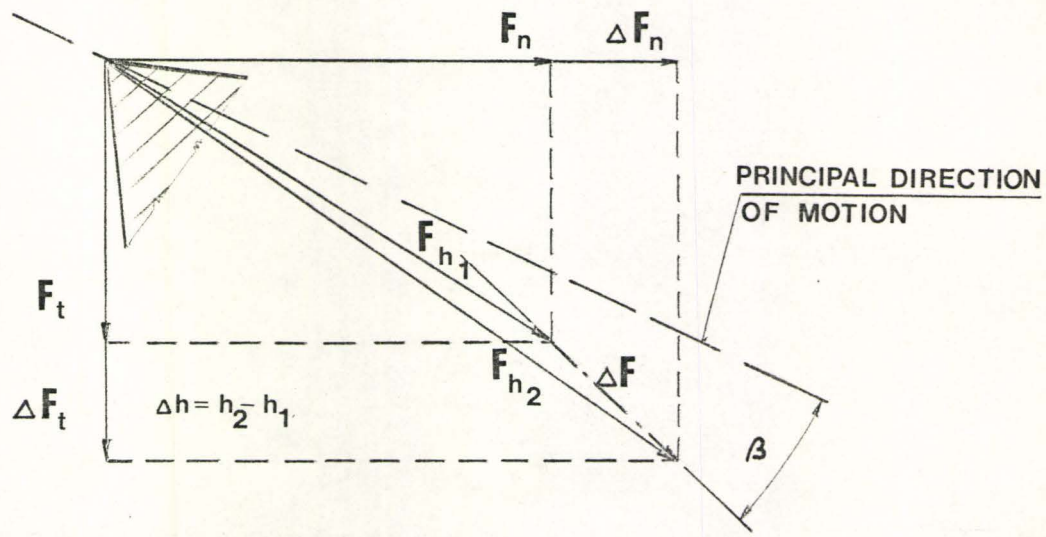

Fig. 8.1 Determination of the incremental cutting stiffness k_i by Peters and Vanhereck.

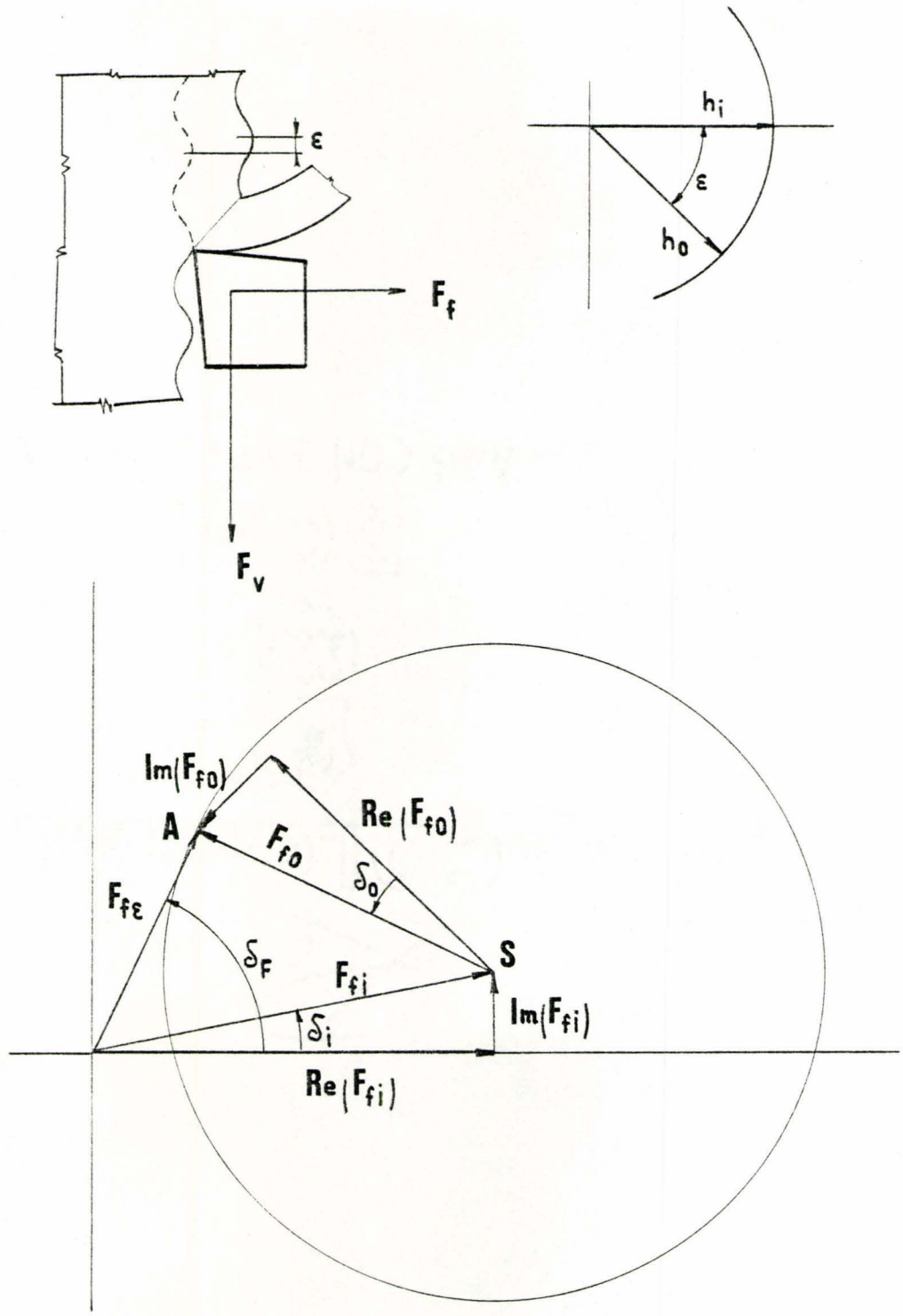

Fig. 8.2 Vector diagram of the dynamic cutting force components by Polacek.

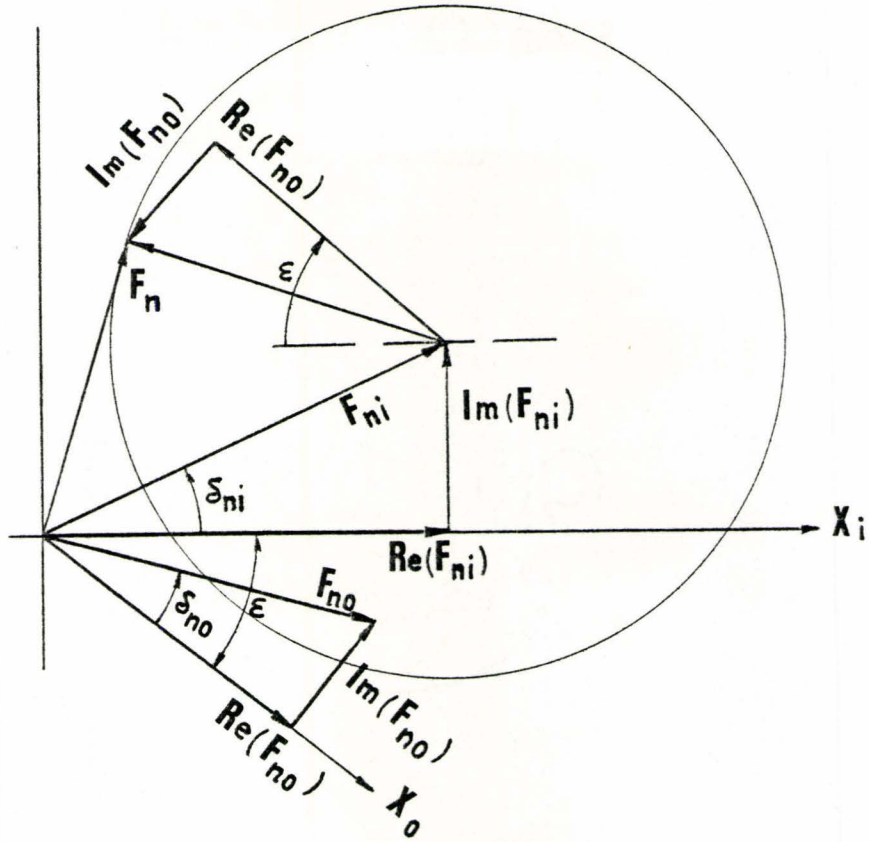

Fig. 8.3a) Vector diagram of dynamic cutting force components by Tlusty and Goel.

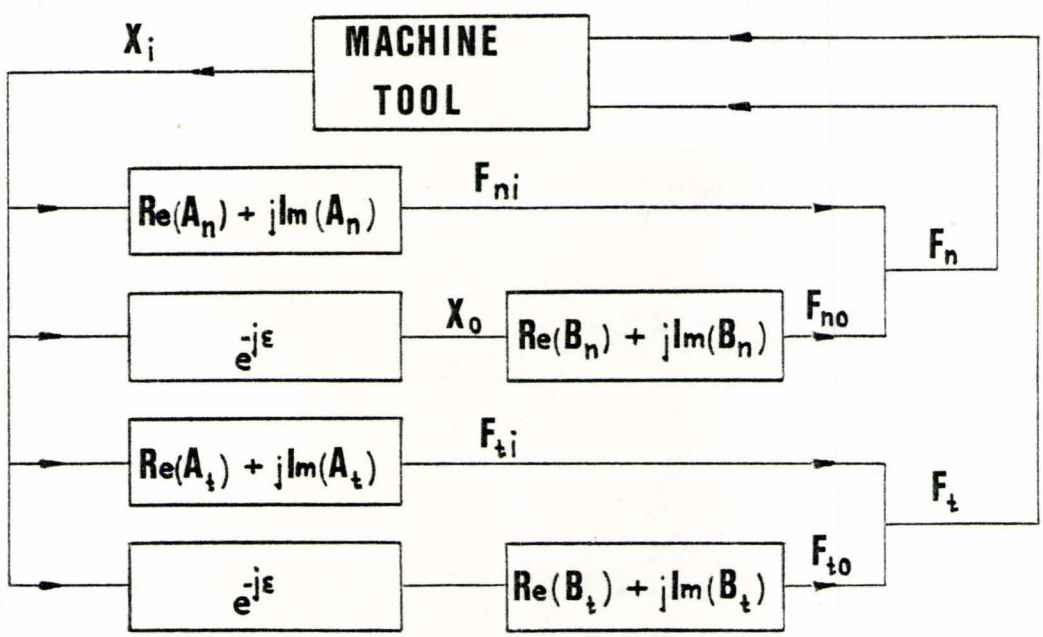

Fig. 8.3b) Block diagram of the dynamic cutting process by Tlusty and Goel.

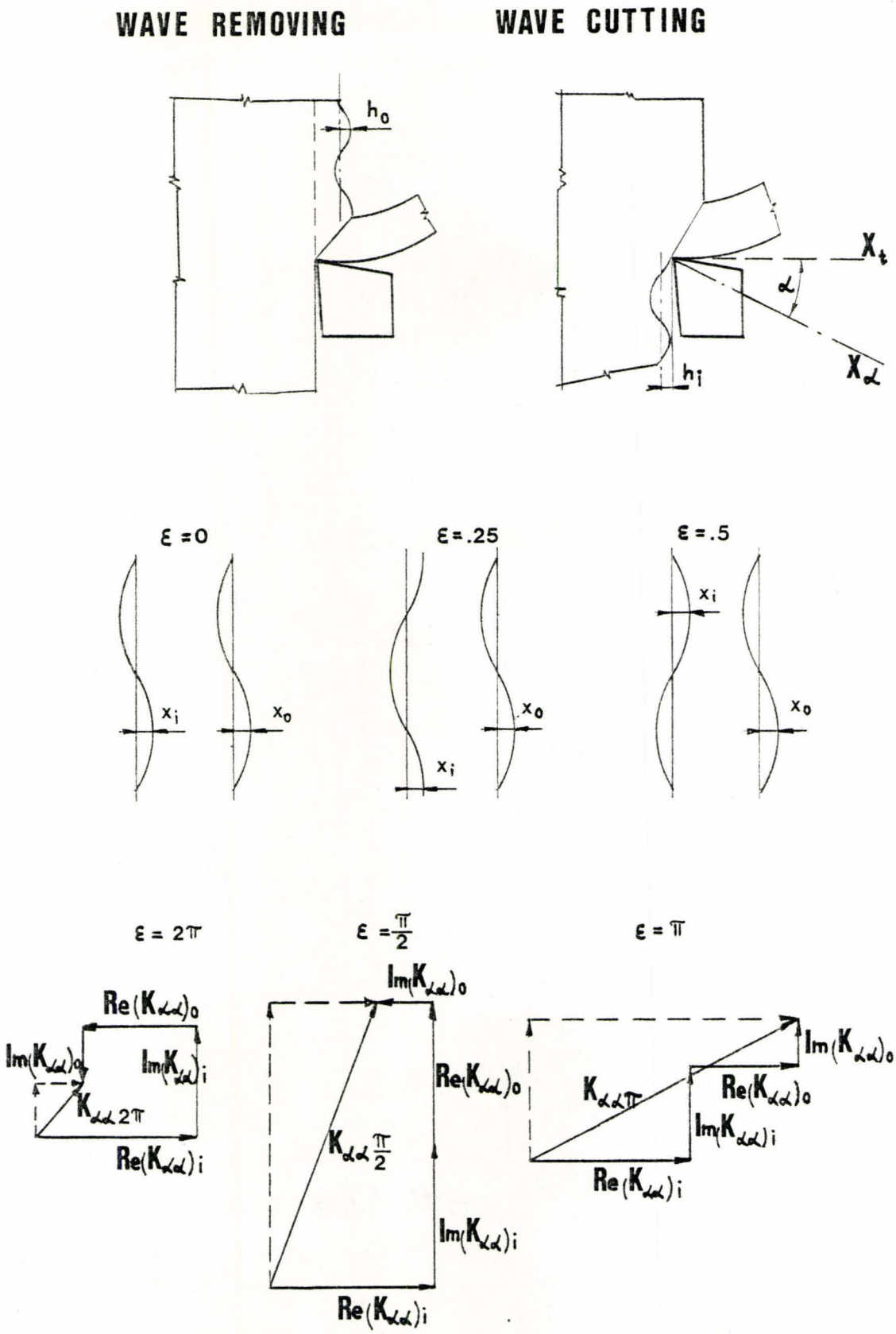

Fig. 8.4. Measurements of DCFC's by Peters, Vanhereck and van Brussel.

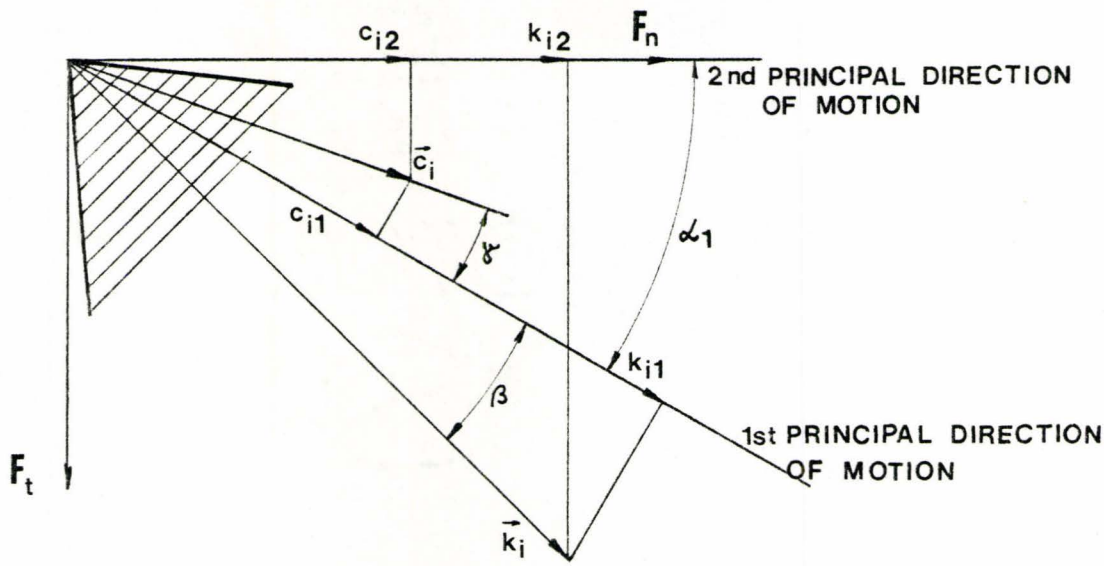

Fig. 8.5 The composition of k_i and c_i.

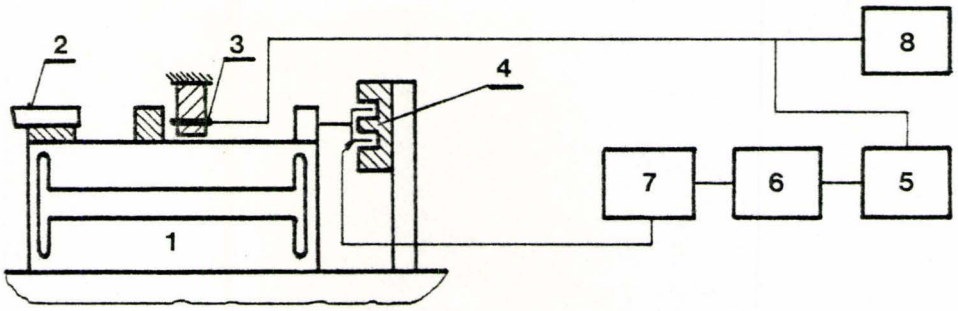

1. Test rig
2. Tool
3. Capacitive probe
4. Electromagnetic exciter
5. Wayne Kerr bridge
6. Phase shift circuit
7. Power amplifier
8. Visicorder

Fig. 8.6a) Measurement set-up

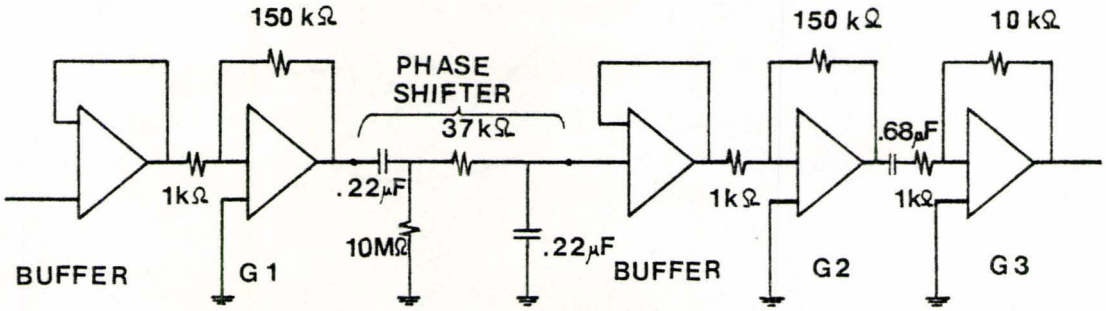

TOTAL GAIN = 100

PHASE SHIFT ≅ 90 (200Hz)

Fig. 8.6b) Phase shift circuit.

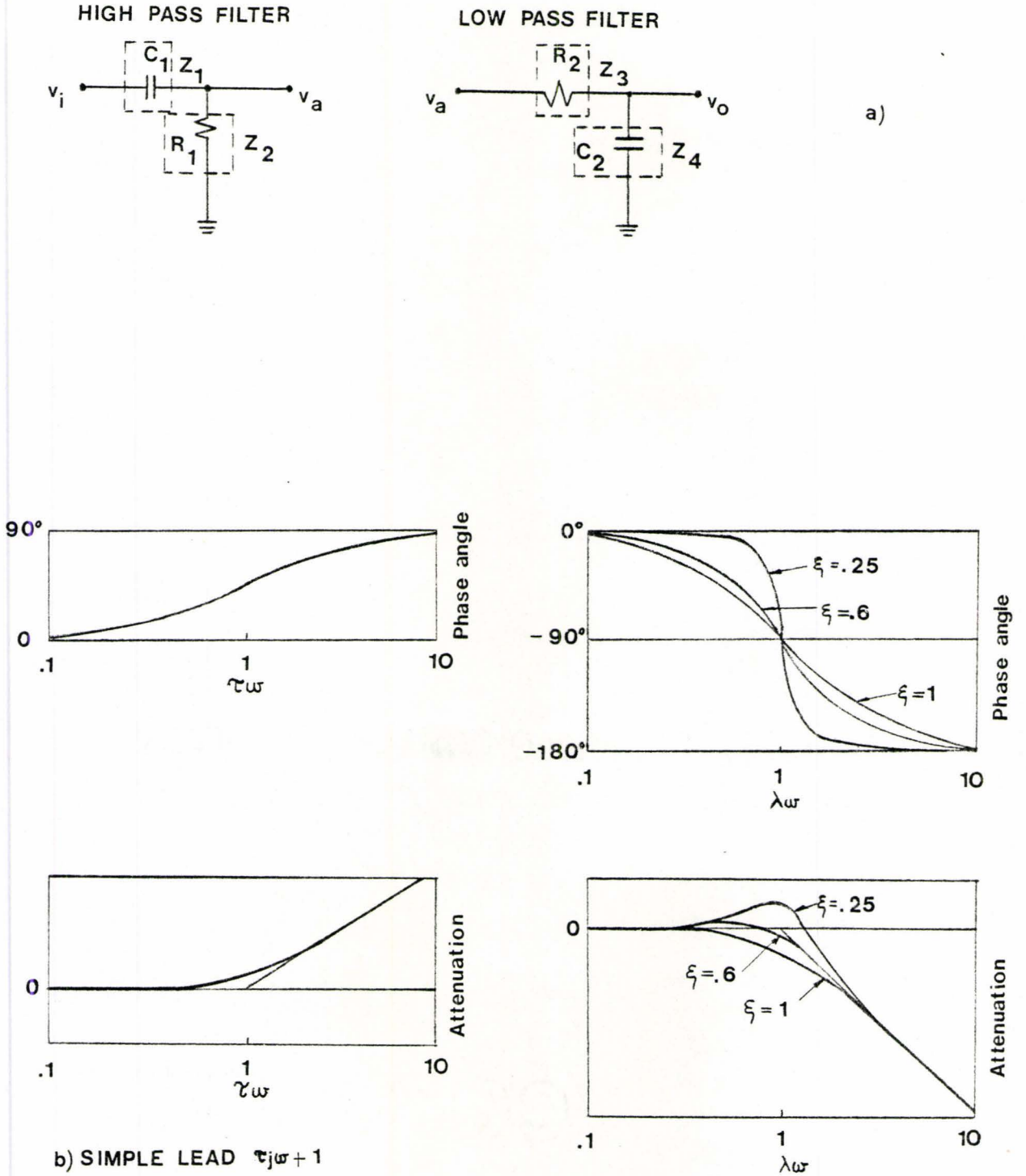

Fig. 8.7 Bode diagrams

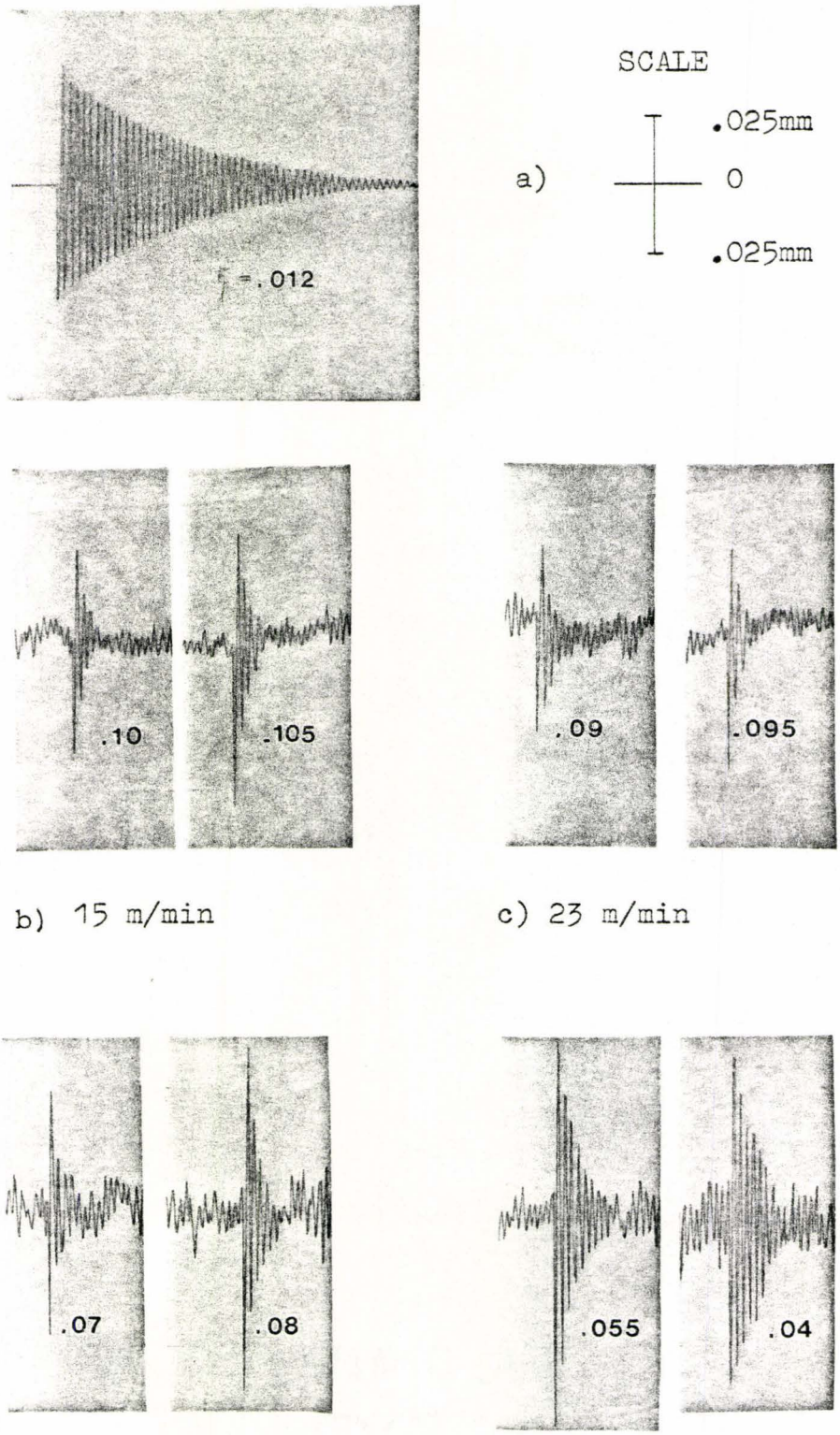

b) 15 m/min

c) 23 m/min

d) 31 m/min

e) 45 m/min

Fig. 8.8 Records from tests

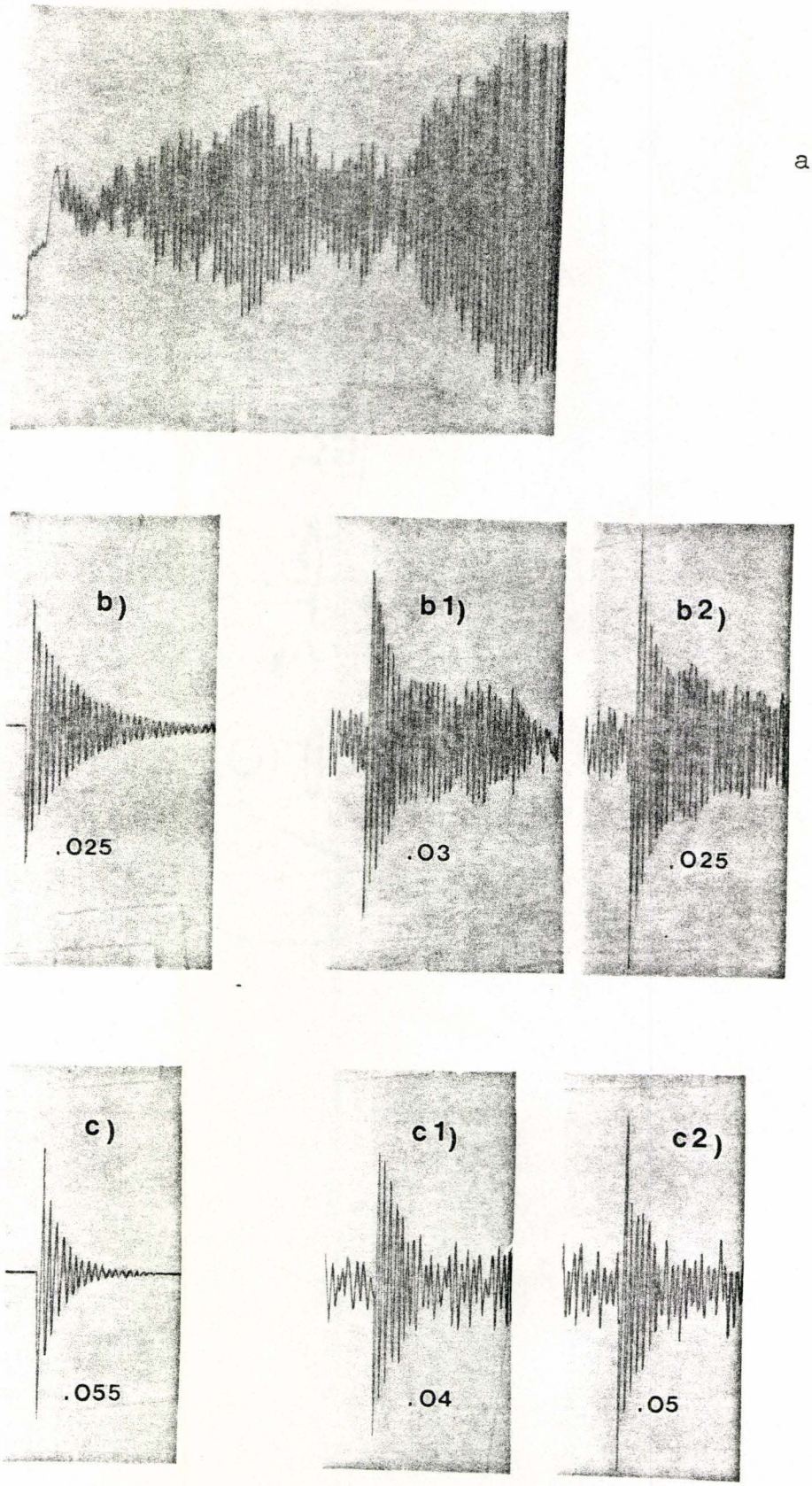

64m/min

Fig. 8.9 Records from tests

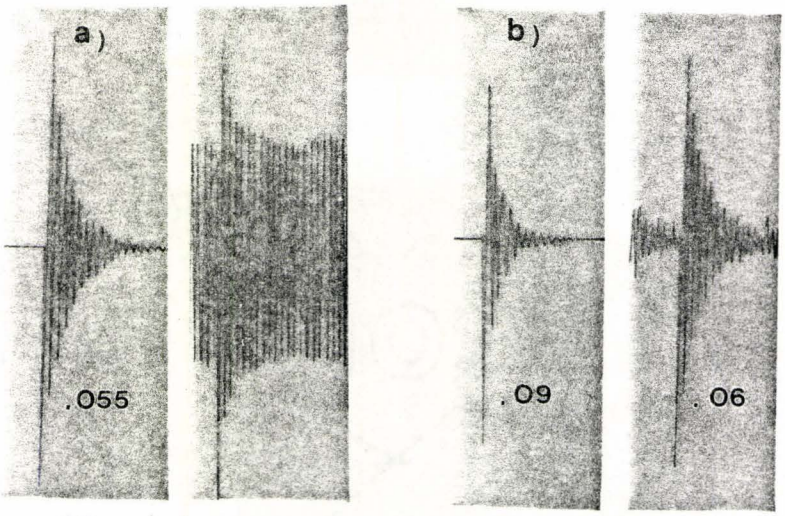

90 m/min

90 m/min

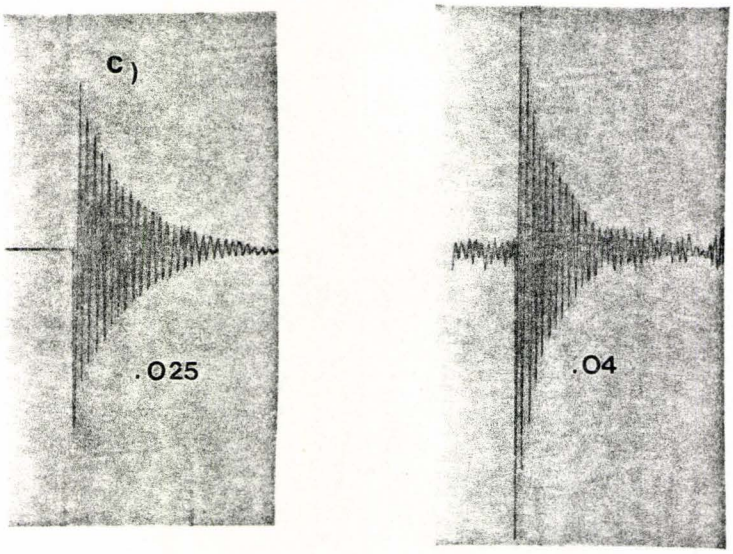

126 m/min

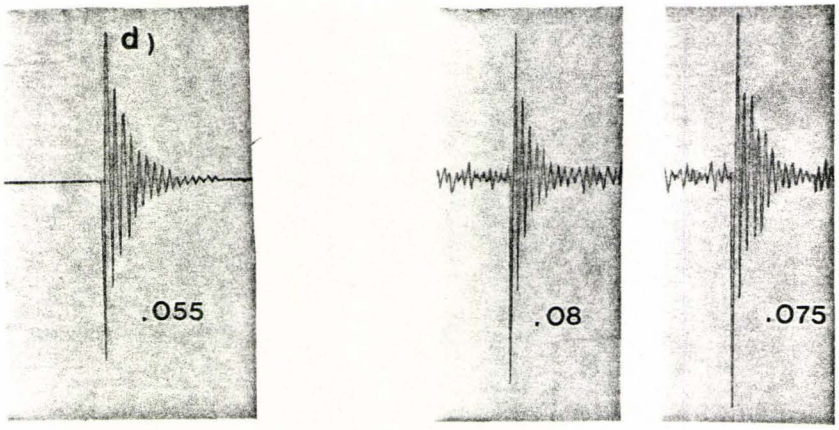

180 m/min

Fig. 8.10 Records from tests

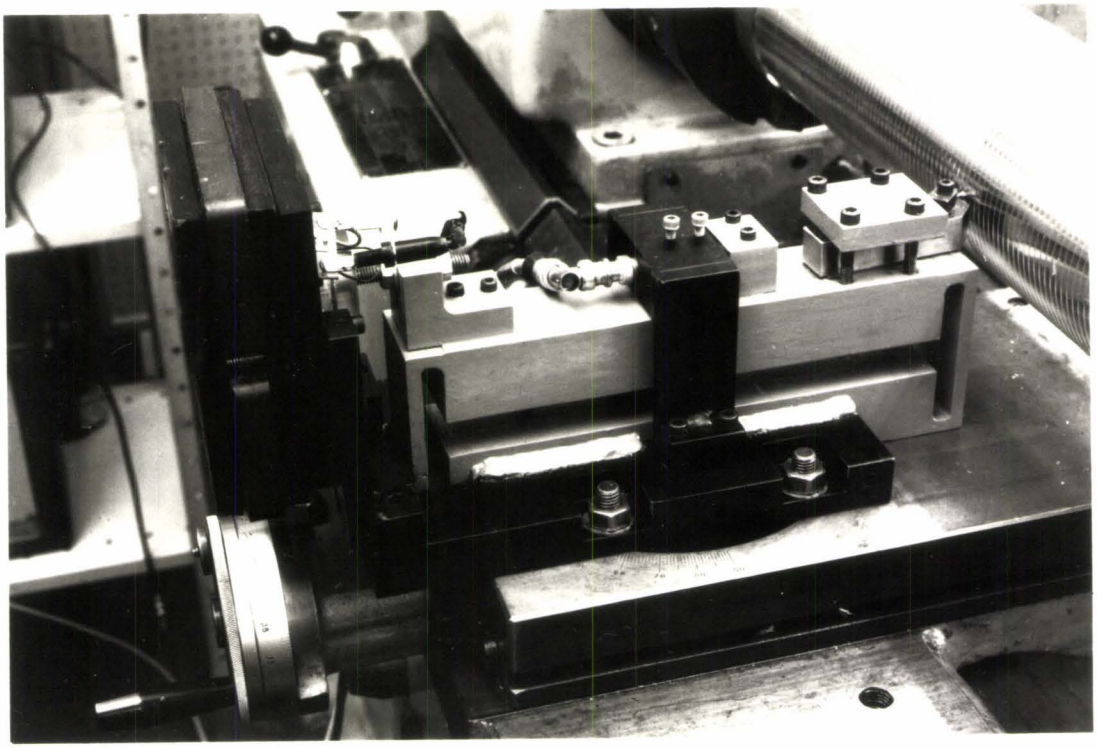

Fig. 8.11a) Test rig

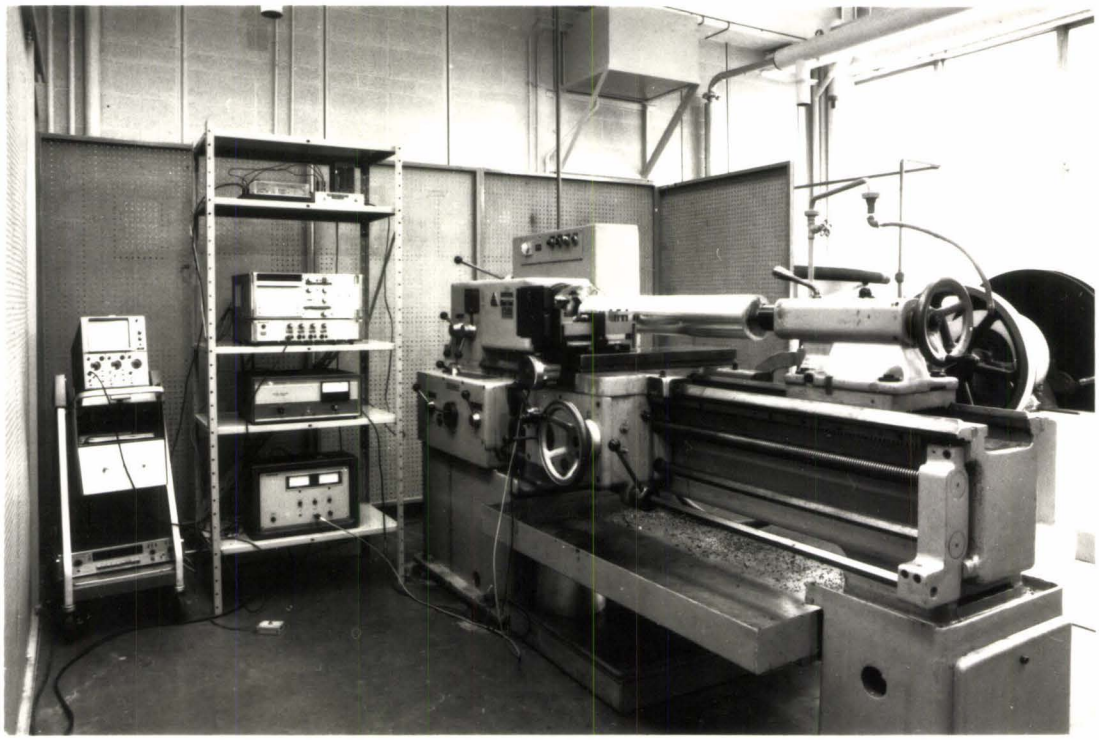

Fig. 8.11b) Test rig and the measurement set-up

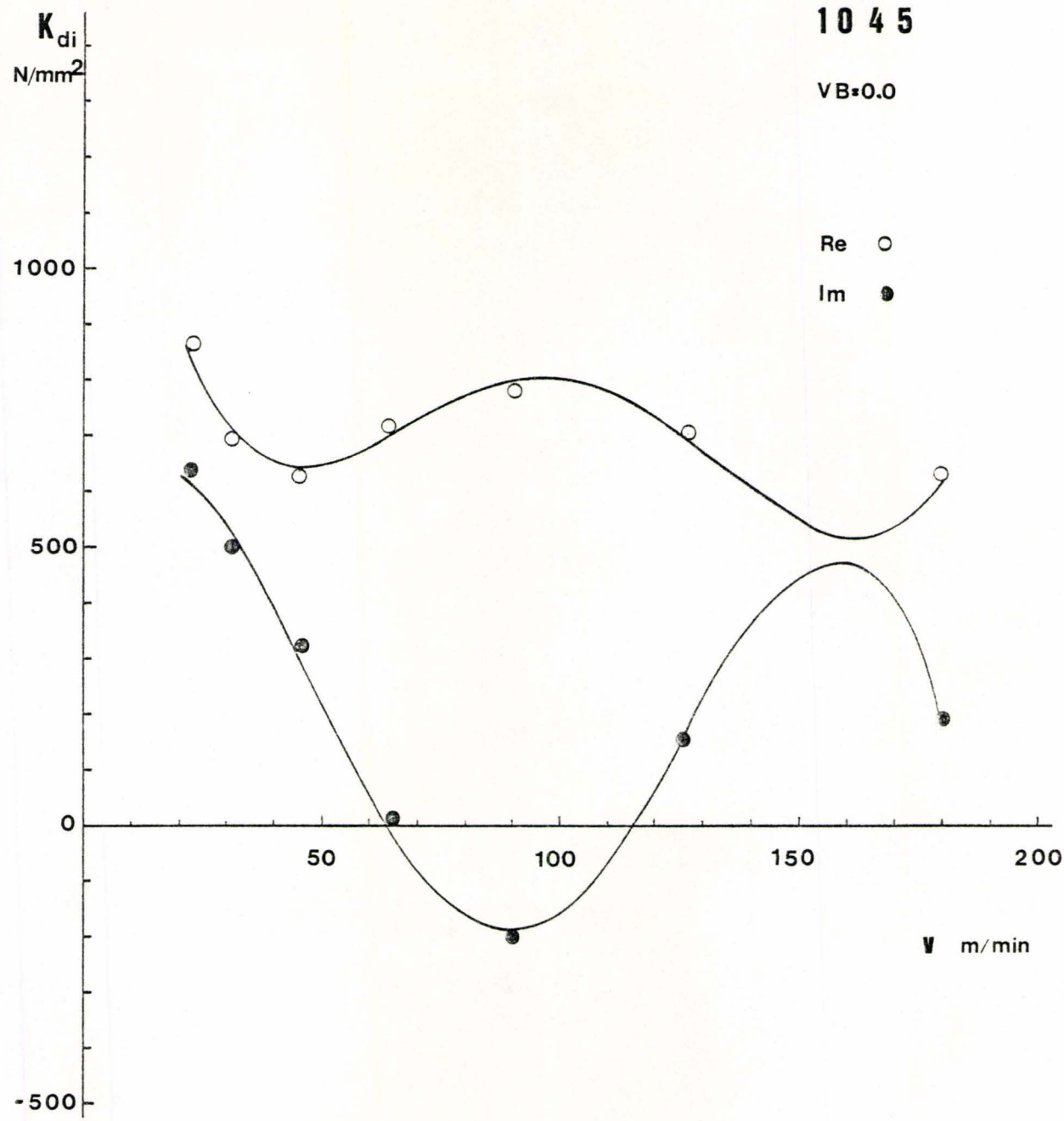

Fig. 8.12 DCFC's versus speed

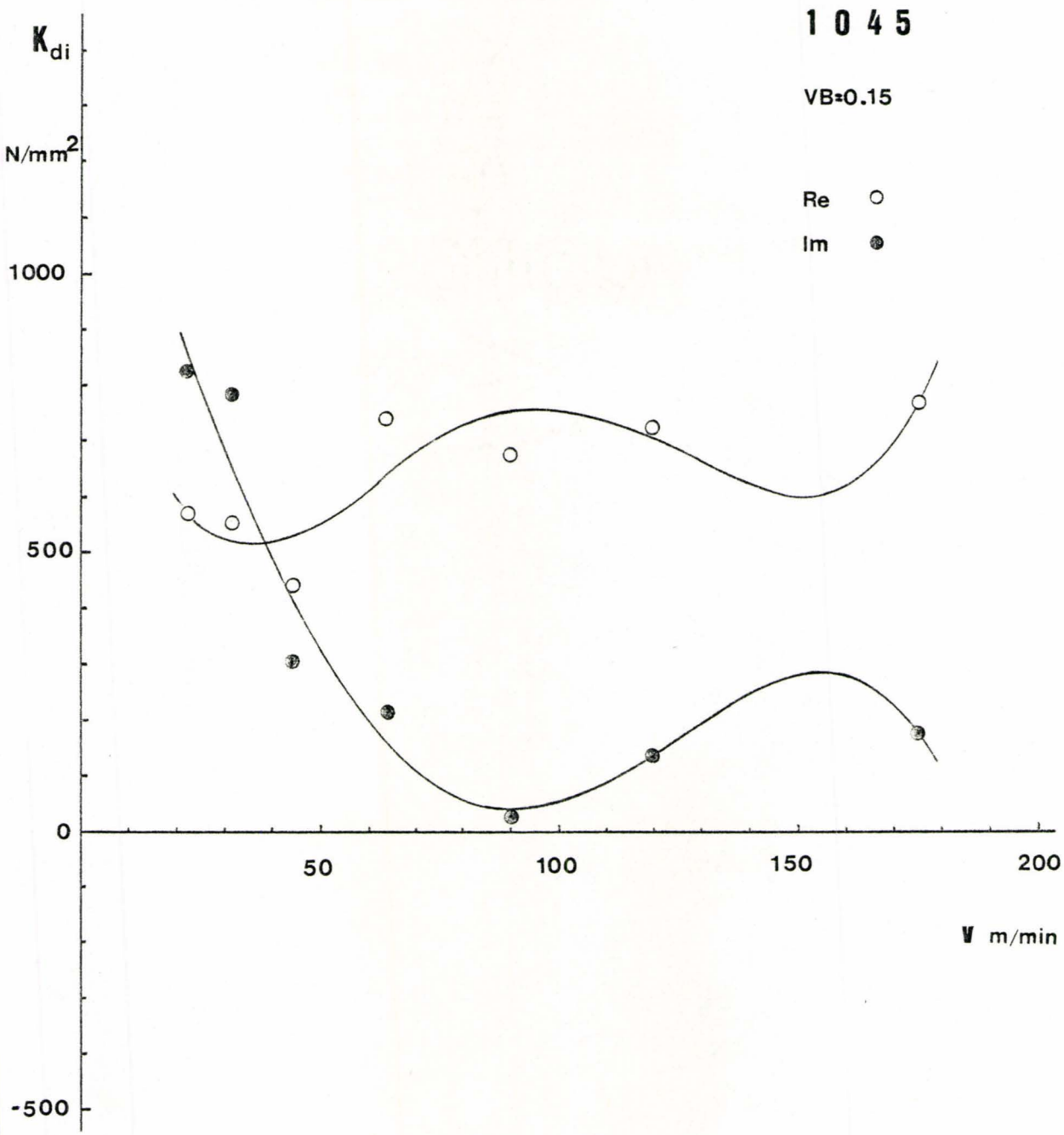

Fig. 8.13 DCFC's versus speed

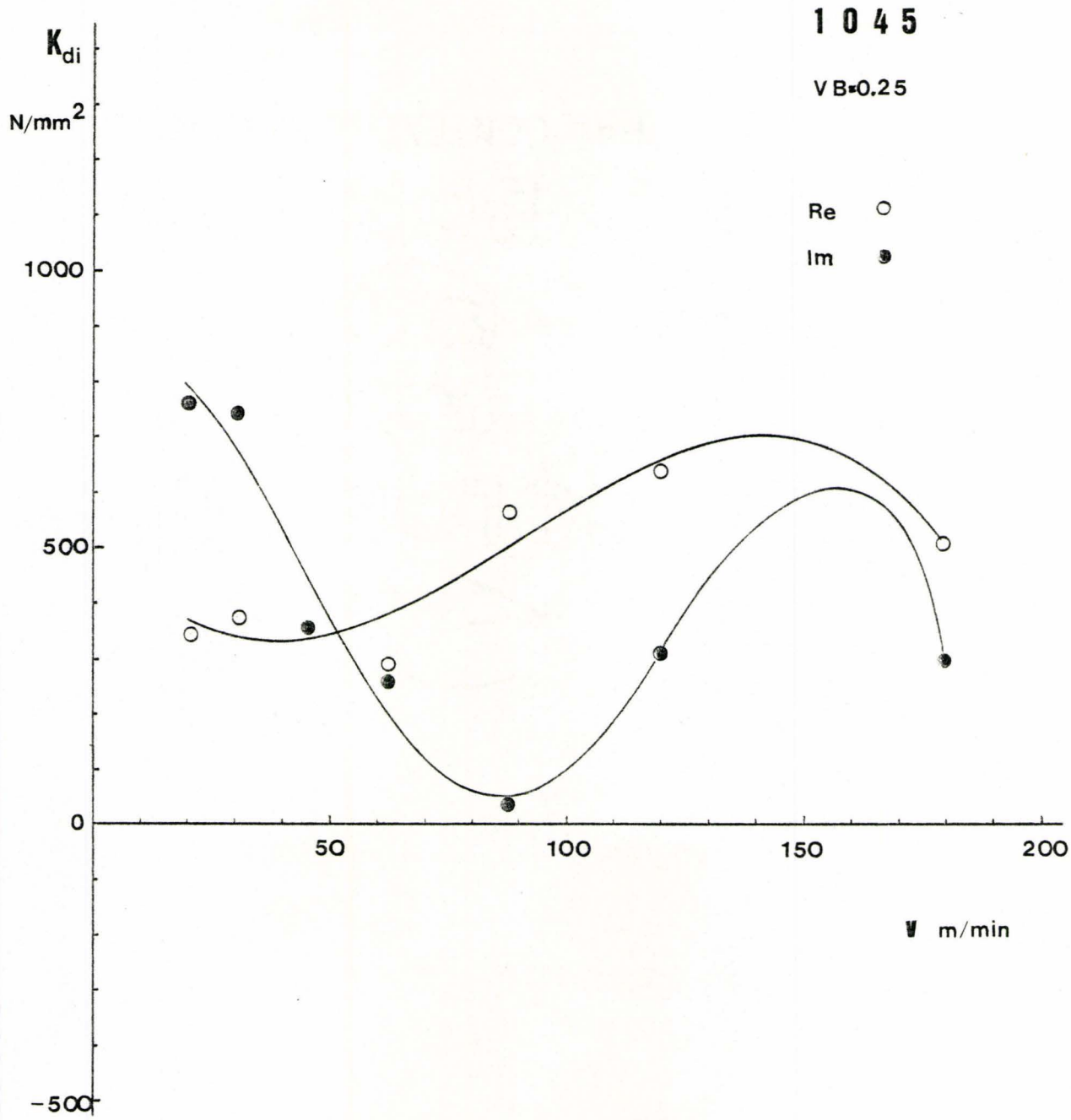

Fig. 8.14 DCFC's versus speed

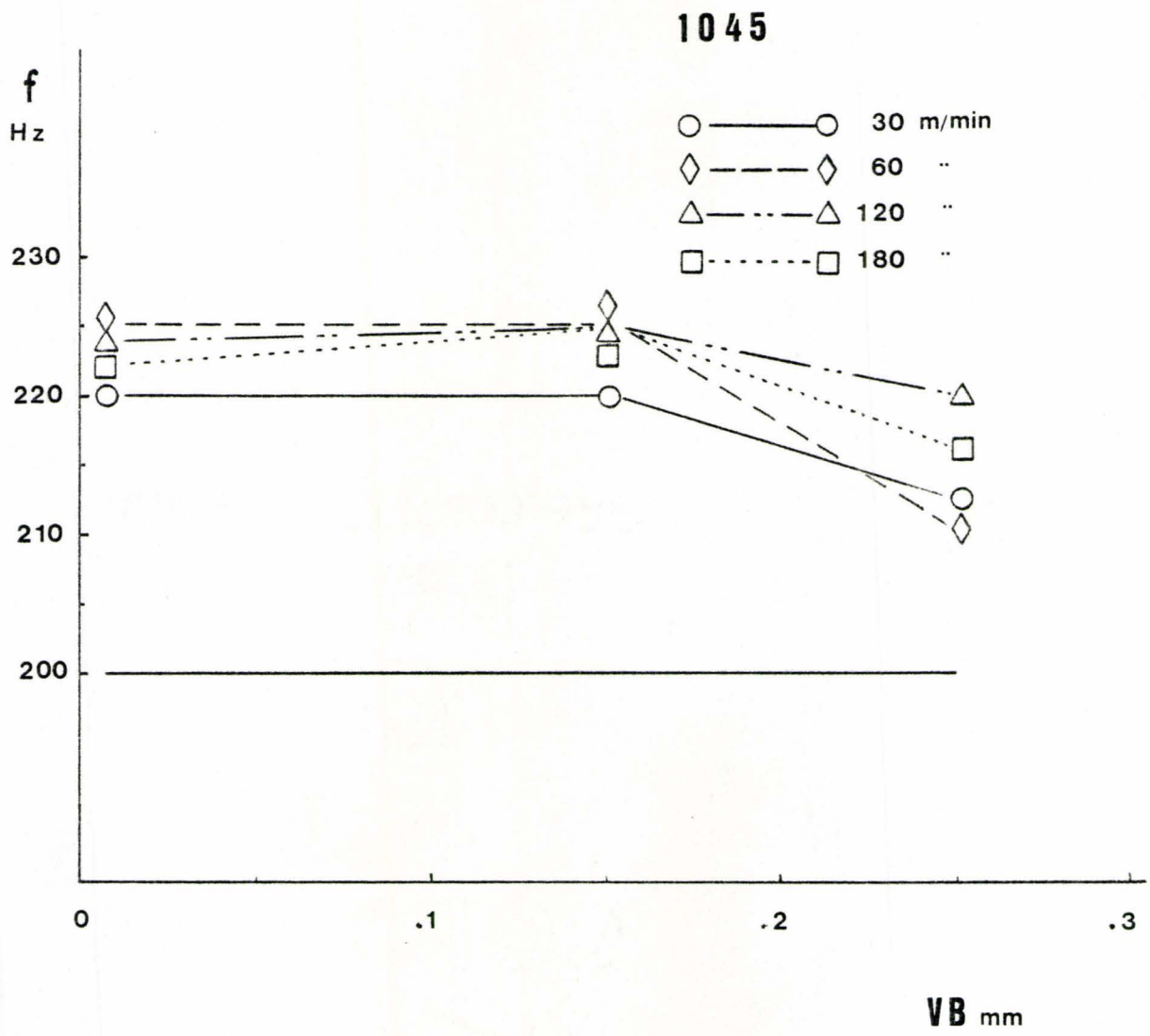

Fig. 8.15 Cutting frequency versus flank wear

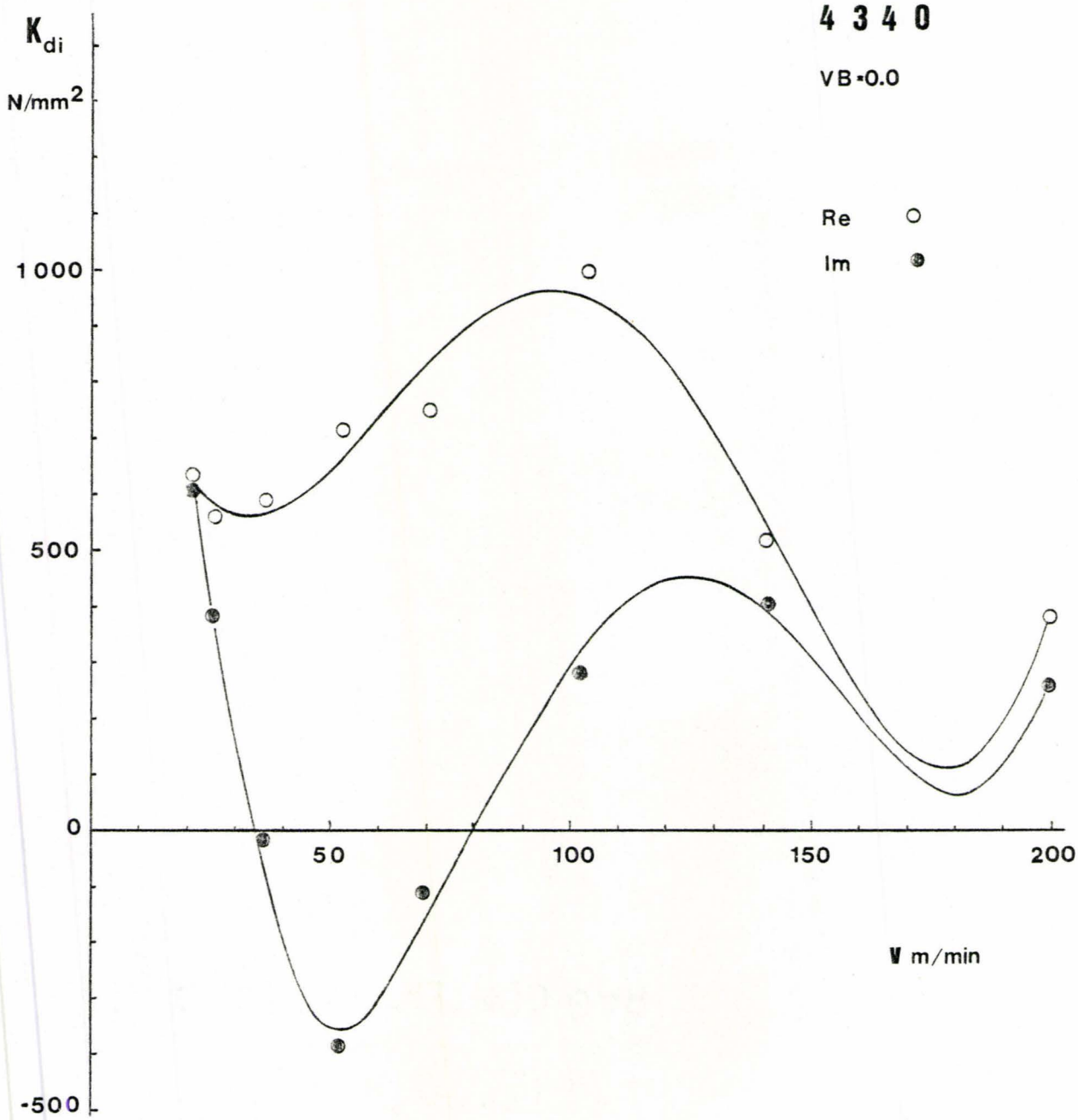

Fig. 8.16 DCFC's versus speed

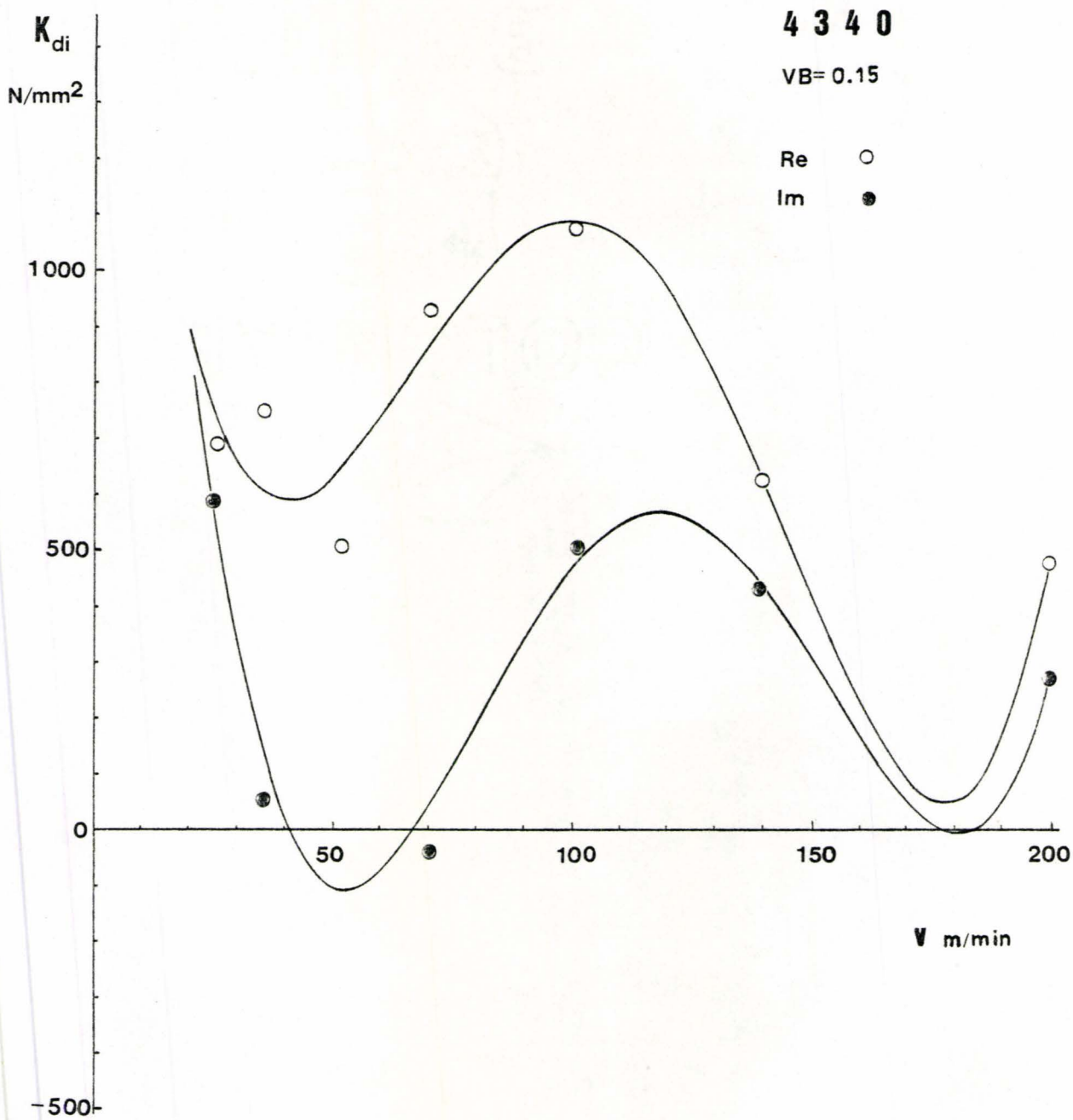

Fig. 8.17 DCFC's versus speed

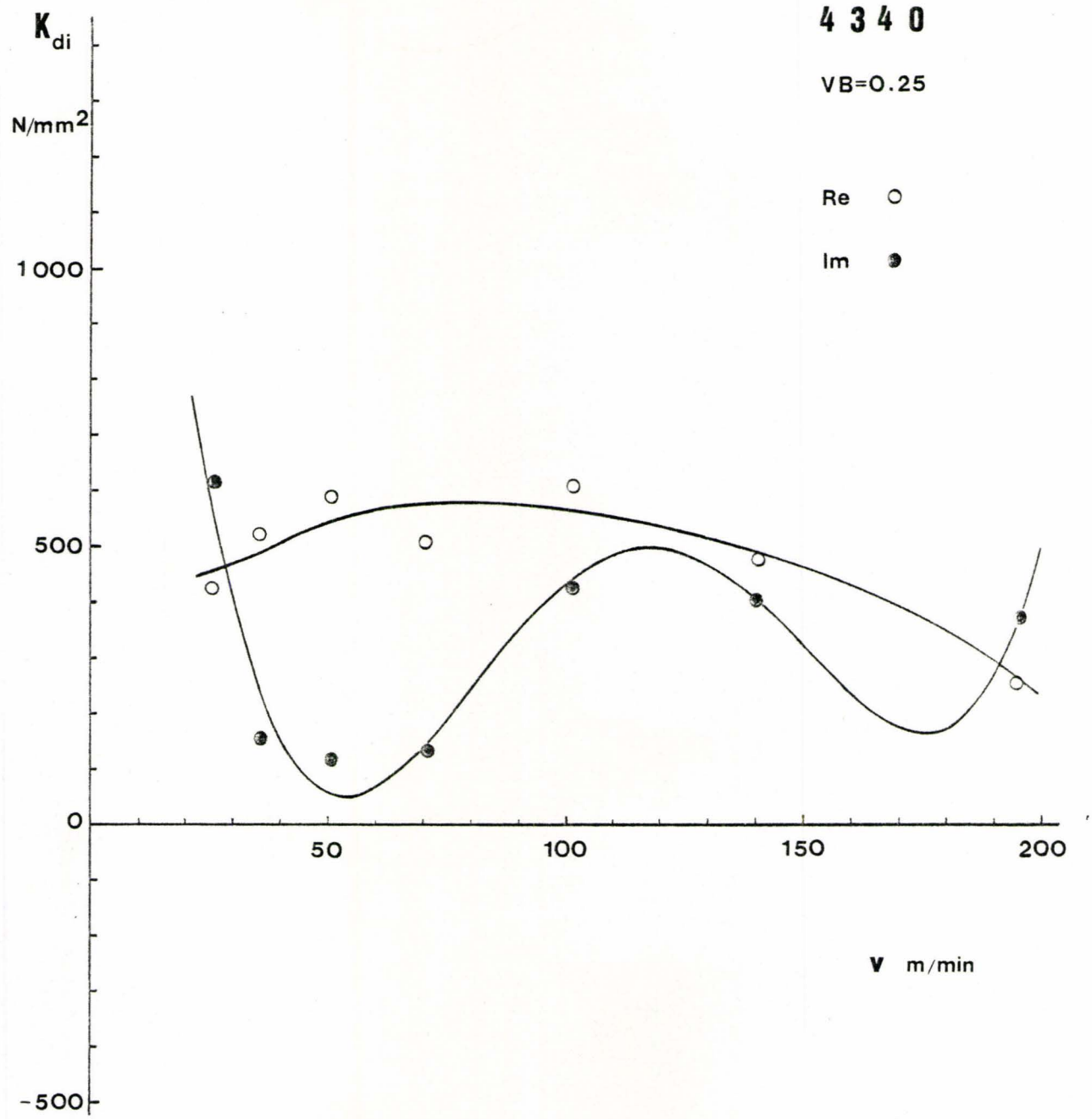

Fig. 8.18 DCFC's versus speed

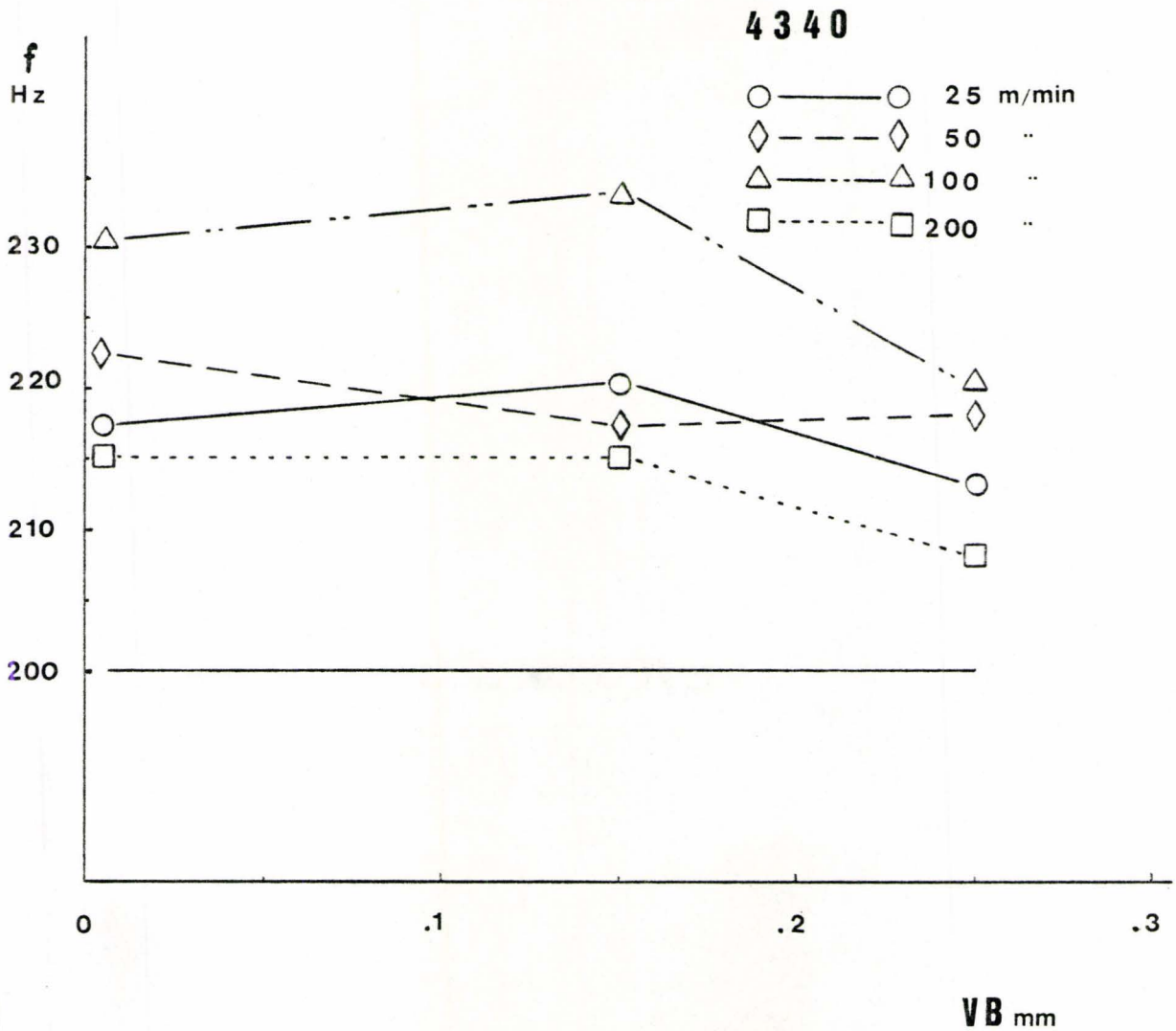

Fig. 8.19 Cutting frequency versus flank wear

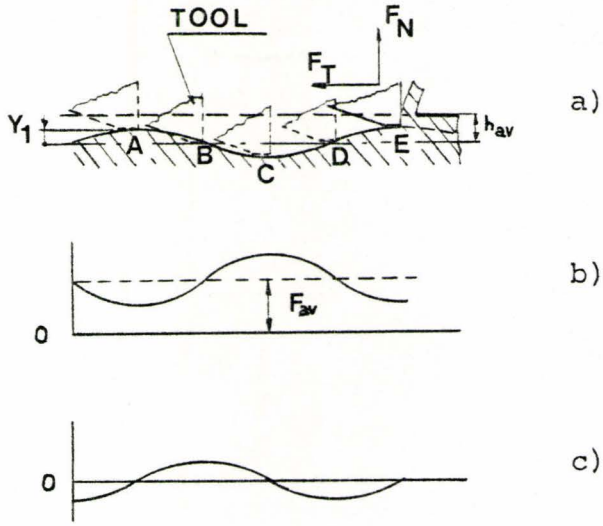

Fig. 8.20 The effect of flank interference on inner modulation coefficient.

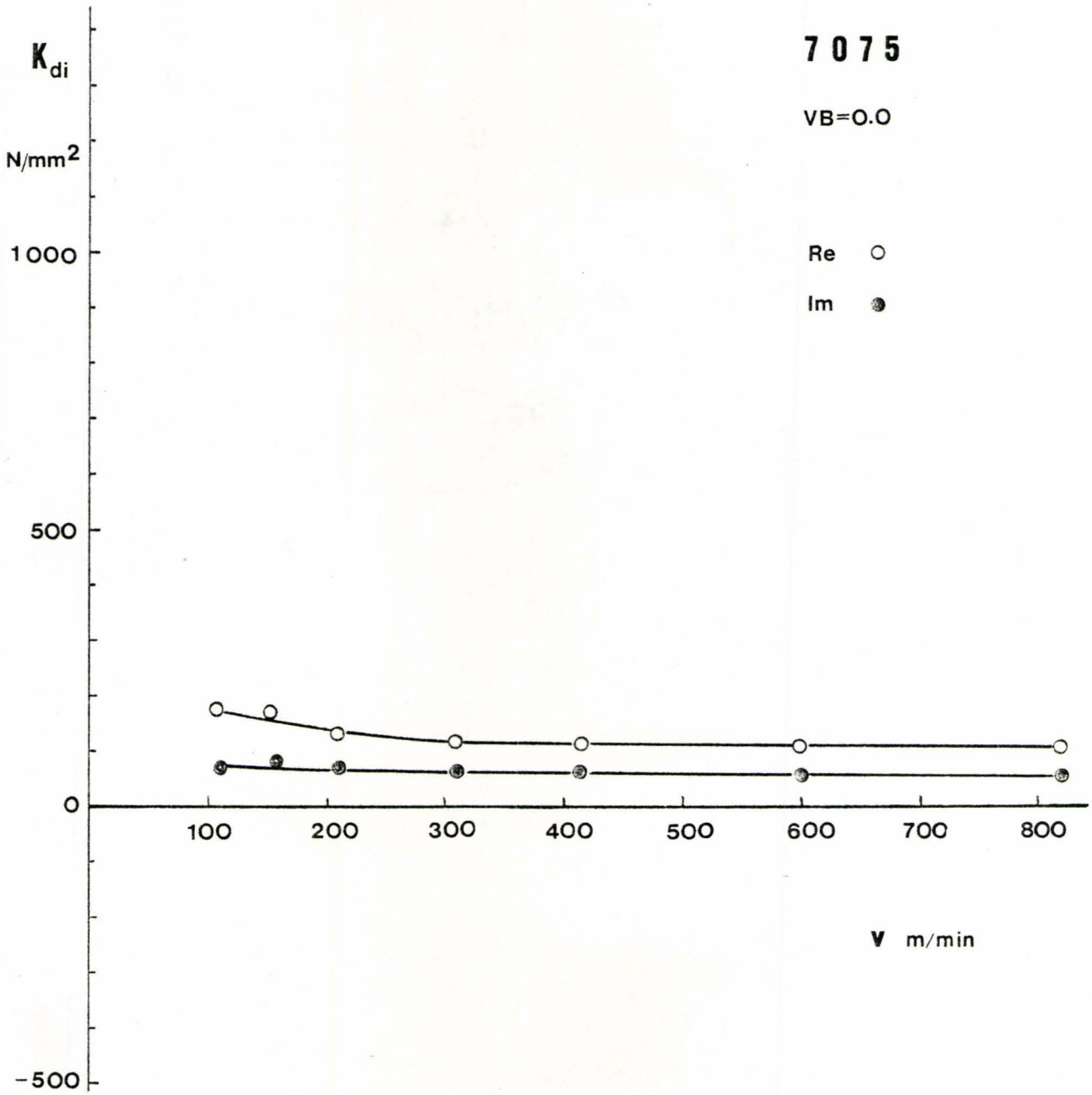

Fig. 8.21 DCFC's versus speed

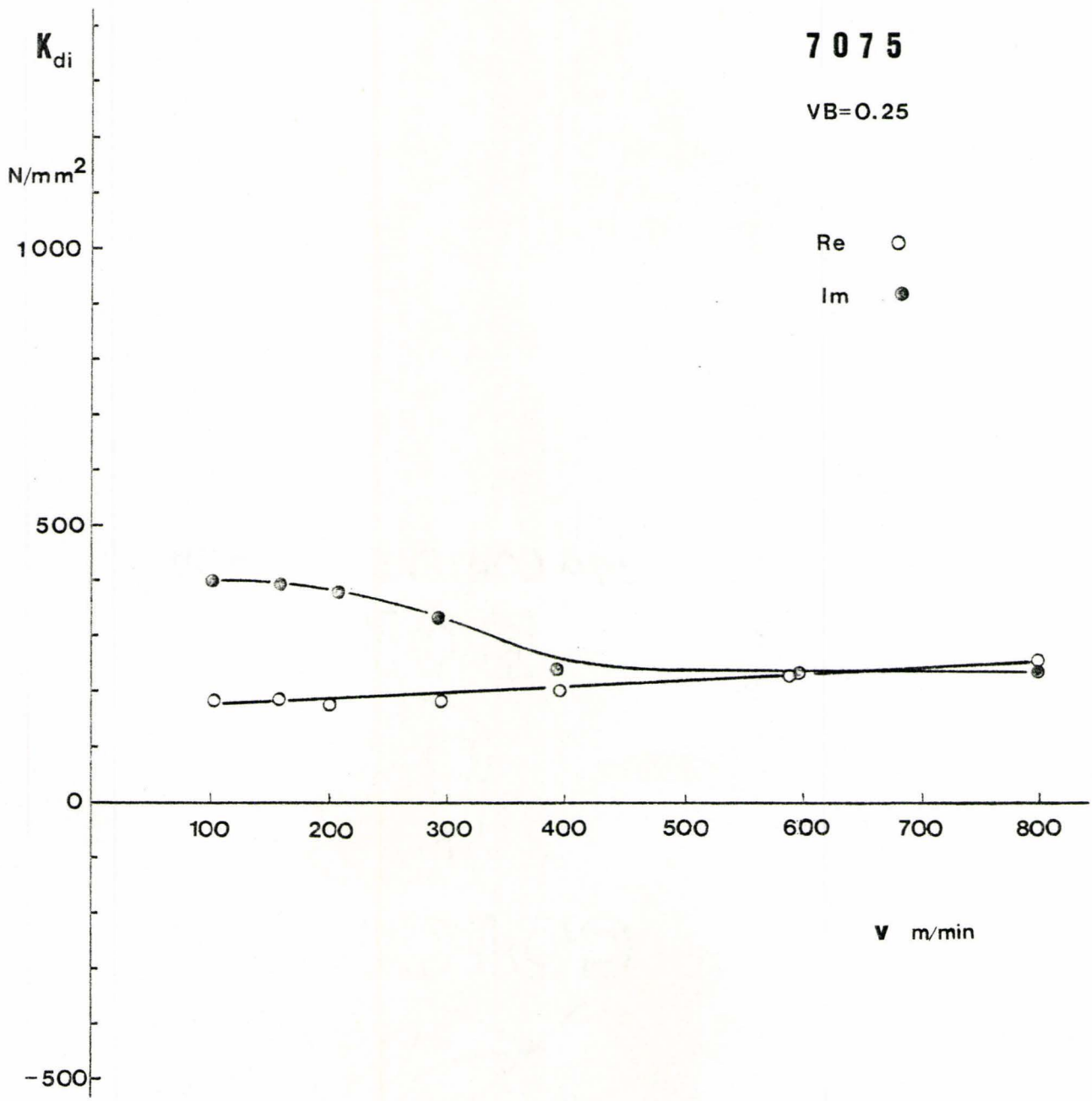

Fig. 8.22 DCFC's versus speed

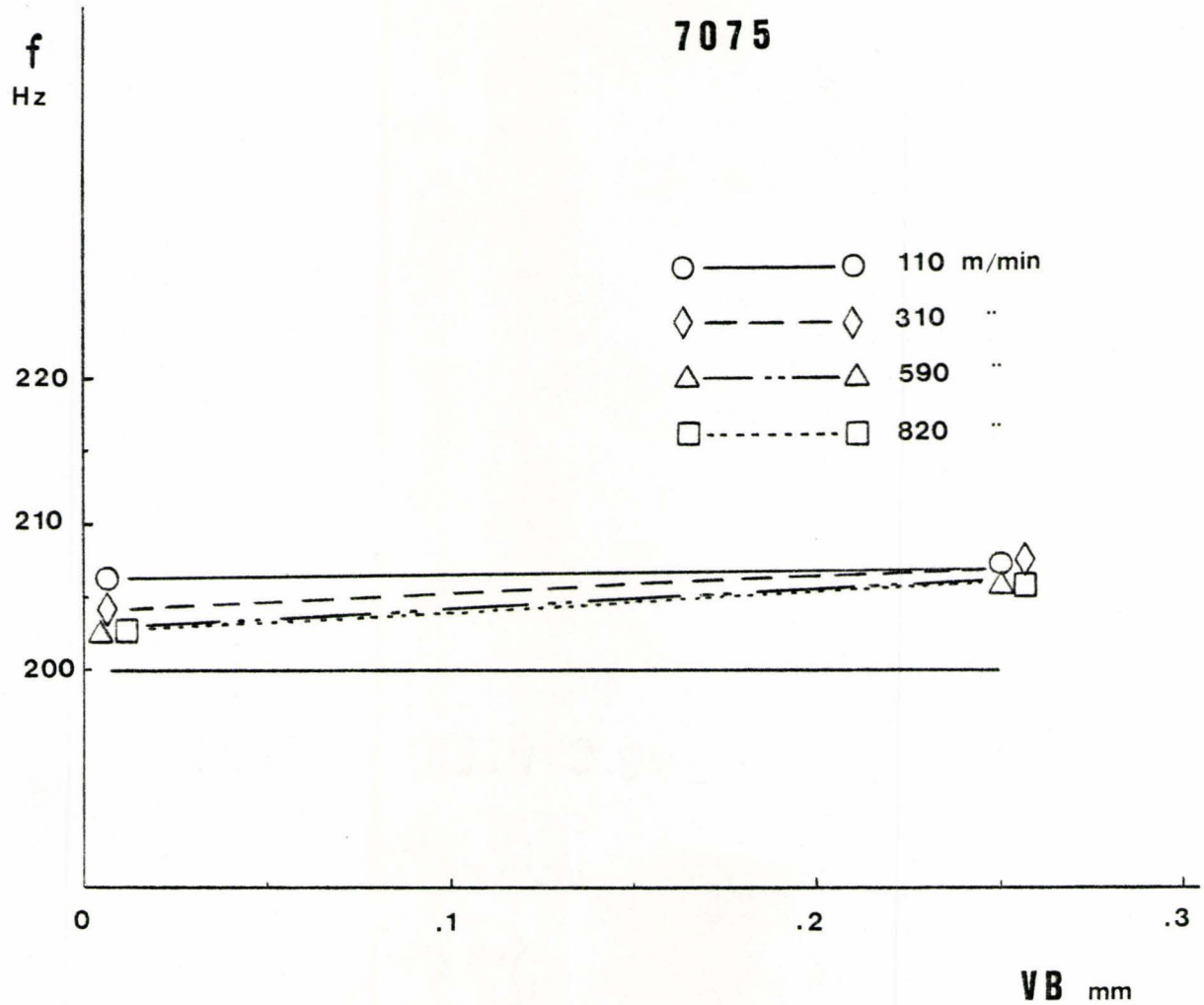

Fig. 8.23 Cutting frequency versus flank wear

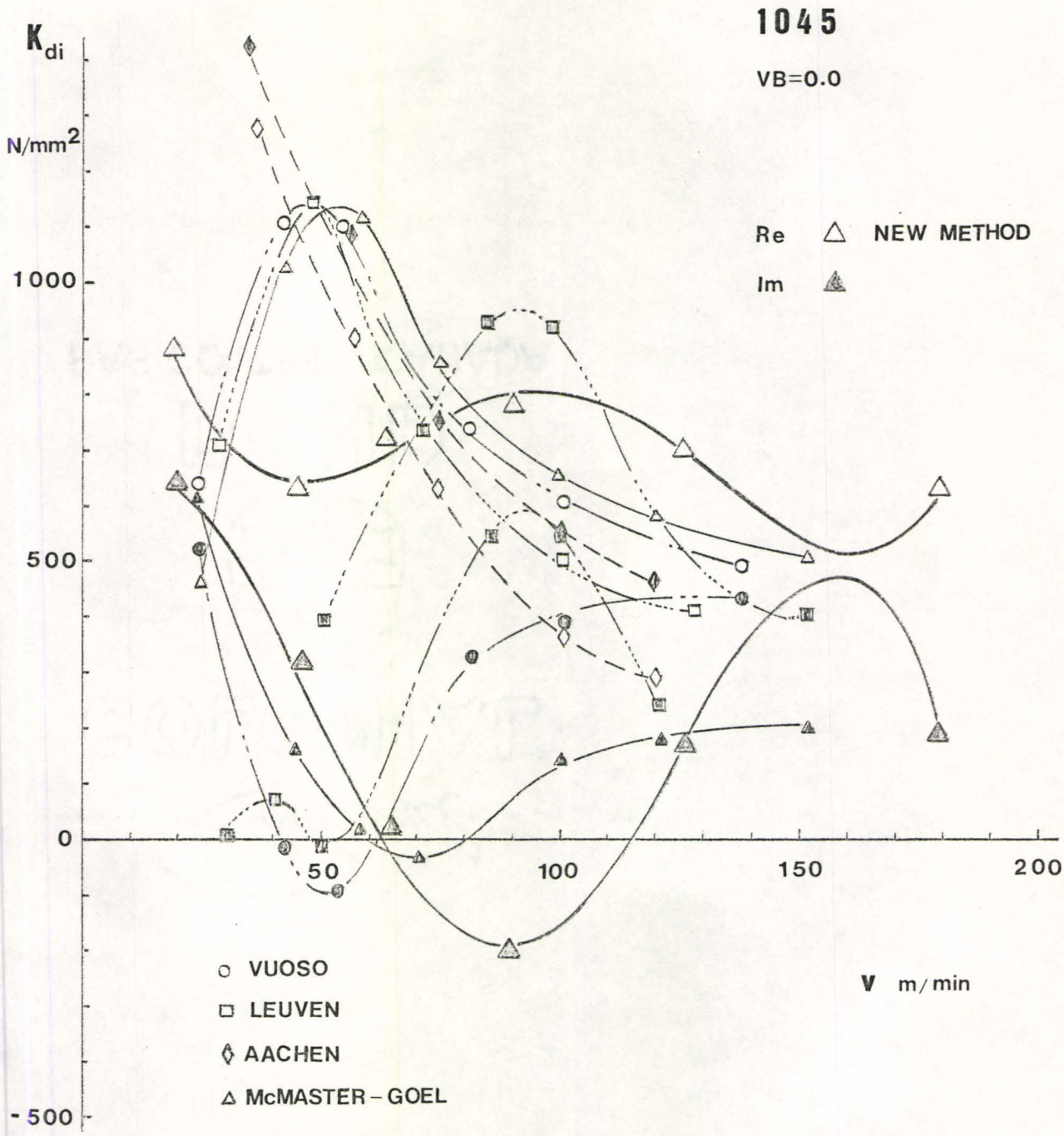

Fig. 8.24 Comparison of DCFC data from various laboratories

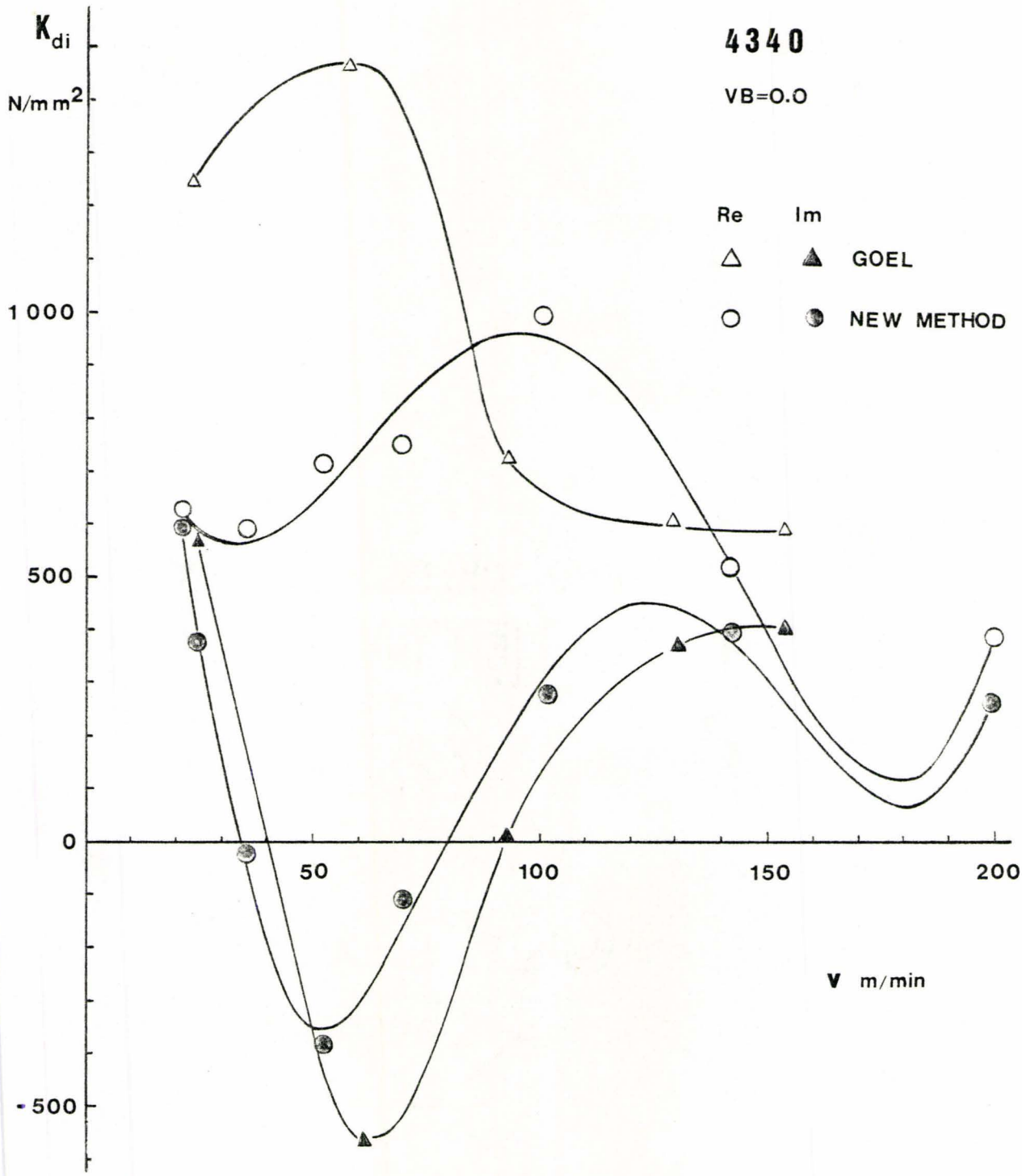

Fig. 8.25 Comparison of DCFC data measured on McMaster

APPENDIX

Power needed to overcome damping, ξ = 10%

Mass of the rig 4.82 kg

Natural frequency of the rig f = 200 Hz

The stiffness of the rig is:

$$k = m\omega^2 = \frac{4.82}{9.81} 2\pi 200 = 7.76 \times 10^3 \text{kg/cm}$$

The critical damping:

$$C_{cr} = 2\sqrt{km} = 12.35 \text{ kg sec/cm}$$

The damping ratio of the system ξ = 0.1 and the amplitude of vibration A = 3.5×10^{-3}cm.

The damping of the system is:

$$c = \xi C_{cr} = 1.235 \text{ kg sec/cm}$$

The damping force:

$$F_d = c \cdot v = c.A.2\pi.f = 5.43 \text{ kg}$$

Power needed to overcome the damping force and maintain the vibration with amplitude A is:

$$p = F_d\ v = 17.05 \text{ kg cm/sec}$$
$$= 1.67 \text{ W}$$

LIST OF REFERENCES

1. Koneigsberger, F. and Tlusty, J.,
   Machine Tool Structures, Vol.1, Pergamon Press, 1970
2. Tlusty, J.,
   Specifications a Tests of Metal Cutting Machine Tools, Proc. of the Conferance, UMIST, 1970
3. Tlusty, J., Morawaki, T, and Goel, B.S.,
   The Dynamic Cutting Force Coefficients for some Carbon Steels, 4th NAMRC., Bathelle' Labs., Colombus, 1976
4. Tlusty, J., and Rao, S.B.,
   Verification and Analysis of Some Dynamic Cutting Force Coefficients Data, 6th NAMRC., U of Florida, 1978
5. Kals, H.J.J.
   On the Calculation of Stability Charts on the Basis of the Damping and the Stiffness of the Cutting Process, CIRP Annuals, 19, 1971, p. 297
6. Kals, H.J.J.
   Dynamic Stability in Cutting, Ph.D. Thesis, U. of Eindhoven 1972
7. Tlusty, J.,
   Analysis of the State of Research in Cutting Dynamics, CIRP Annuals, 27/2, 1978
8. Tlusty, J. and Polacek, M.,
   Beispiele der Behandling der selbsterregten Sckwingungen der Werkzeuge Machinen.

Proc. 3rd Forschungs - und Konstruktion - Collequium Werkzeug - machine und Betriebwissen shaft (1957)

9. Opitz, H. and Wentze, G.
Application of a Process Controll Computer for Measurement of Dynamic Cutting Coefficients, Laboratorium für Werkzeug machinen U, Betriebslehrc Tech. Hochschule Aachen, 1972

10. Polacek, M.,
Report to Ma group CIRP, VUOSO Praha, 1969

11 Peters, J., Vanhereck, P., van Brussel, H.,
The Measurement of the Dynamic Cutting Coefficients, CIRP Annuals, p.129, 1971

12. Tlusty, J. and Goel, B.S.,
Measurement of the Dynamic Cutting Force Coefficients Proc. of the 2nd NAMRC, 1974

13. Tobias, S.A. and Fischwick, W.,
A Theory of Regenerative Chatter,
The Engineer (London), 1958

14. Das, M.K. and Tobias, S.A.,
The Relation between Static and Dynamic Cutting of Metals.
Int. Journal of Mach. Tool Des. and Res., 1971

15. Peters, J. and Vanhereck, P.
Machine Tool Stability Tests and the Incremental Stiffness, CIRP Annuals 17, 1969

16. Goel, B.S.,
Measurement of Dynamic Cutting Force Coefficients,
Ph.D. Thesis, McMaster Univ., 1976

17. Rao, S.B.,
Analysis of the Dynamic Cutting Force Coefficients
M.Eng. Thesis, McMaster Univ., 1977

18. Dautzenberg, J.H. and Tlusty, J.,
Determination of the Imaginary Part of the Direct
Inner Dynamic Cutting Coefficients with the Kals method,
MRDG Rep. 131, McMaster Univ., 1978

19. Sarnicola, J.F. and Boothroyd, G.,
Machine Tool Chatter: Factors which Influance Cutting
Forces during Wave Removing,
Proc. of the 1st NAMRC, 1973

20. Sarnicola, J.F. and Boothroyd, G.,
Machine Tool Chatter: Effect of Equivalent surface
Slope on Shear Angle during Wave generating and
Regenerative Chatter
Proc. of the 2nd NAMRC, 1974

21. Stewart, U.A. and Brown, R.H.,
The Inter-relationship of Shear and Friction Processes
in Machining under Regenerative Chatter Conditions,
Proc. of Int. Mach. Tool. Des. and Res., 1972

22. Tlusty, J. and Heczko, O.
Improving Tests of Damping in the Cutting Process
Proc. of the 8th NAMRC, 1980